HOLLOW CONCRETE COLUMNS: REVIEW OF STRUCTURAL BEHAVIOR AND NEW DESIGNS USING GFRP REINFORCEMENT

O.S. AlAjarmeh[1,*], A.C. Manalo[1], B. Benmokrane[2], K. Karunasena[1], W. Ferdous[1], P. Mendis[3]

[1] University of Southern Queensland, Centre for Future Materials (CFM), School of Civil Engineering and Surveying, Toowoomba 4350, Australia
[2] University of Sherbrooke, Department of Civil Engineering, Sherbrooke, Quebec, Canada
[3] The University of Melbourne, Department of Infrastructure Engineering, Victoria 3010, Australia
Email: Omar.Alajarmeh@usq.edu.au; Allan.Manalo@usq.edu.au; Brahim.Benmokrane@USherbrooke.ca; Karu.Karunasena@usq.edu.au; Wahid.Ferdous@usq.edu.au; Pamendis@unimelb.edu.au

ABSTRACT

Hollow concrete columns (HCCs) reinforced with steel bars have been employed extensively for bridge piers, ground piles, and utility poles because they use fewer materials and offer higher structural efficiency compared to solid concrete columns with the same concrete area. Many experimental studies have been conducted to investigate the behavior of HCCs under different loading conditions and found that the structural performance of HCCs is critically affected by many design parameters. If not designed properly, HCCs exhibit brittle failure behavior, due to longitudinal bars buckling or the concrete wall failing in shear. In addition, the corrosion of steel bars has become an issue in reinforced-concrete structures. Therefore, this paper critically reviews the different design parameters that affect the performance of HCCs and identifies new opportunities for the safe design and effective use of this construction system. Moreover, the use of GFRP bars as reinforcement in hollow concrete columns is explored with the aim of developing a non-corroding and structurally reliable construction system.

Keywords: Hollow concrete column, axial-load ratio, inner-to-outer diameter ratio, steel, GFRP, ductility, confined strength.

INTRODUCTION

Steel-reinforced hollow concrete columns (HCCs) have been used for bridge piers, piles, and utility poles due to their enhanced structural efficiency and their higher strength- and stiffness-to-mass ratios than solid concrete columns (SCCs) with the same cross-section area [1, 2]. Creating a hollow section reduces the amount of materials used in the columns and minimizes the self-weight, thereby leading to an efficient construction system. The structural behavior of HCCs with steel reinforcement under different loading conditions has been extensively investigated [1-15]. This type of column is profoundly affected by several design parameters,

including the axial-load ratio ($\frac{P_o}{f_c' A_c}$) (the ratio between the applied and ultimate axial-load capacities) [3, 4], inner-to-outer diameter (i/o) ratio [5, 6], reinforcement ratio (ρ) [7, 8], volumetric ratio (ρ_v) [9, 10], concrete compressive strength (f_c') [11, 12], aspect ratio (AR) [13, 14], and geometry (G) [2, 15]. These parameters were found more critical in HCCs than the SCCs, owing to the lack of concrete confinement in HCCs compared to SCCs, which leads to crushing of the inner concrete wall and brittle failure.

HCCs have low deformation capacity [14] and experience a sudden reduction in strength [2] resulting in brittle failure behavior. This behavior is normally caused by defective design resulting in the buckling of the reinforcement due to insufficient reinforcement details or crushing of the inner unconfined concrete wall as a result of inadequate concrete strength. The brittle failure of HCCs is also caused by the yielding of longitudinal bars. At this point, the reinforcement can no longer resist, leading to overstressing and crushing of the unconfined concrete wall. Whittaker [5] reported that HCCs with steel reinforcement can be detailed appropriately if the longitudinal bars are held by the concrete wall and confined by lateral reinforcement until failure. Therefore, the design parameters should be carefully considered to ensure HCCs are functional and sustainable, and fail in a ductile manner. The corrosion of steel reinforcement is also becoming a significant challenge with steel-reinforced SCCs and HCCs. The problem is more critical with HCCs than SCCs because their outer and inner surfaces expose more concrete surface area. Therefore, there is a need to explore non-corroding reinforcing options that can overcome the limited strain and strength capacities of HCCs.

Glass fiber-reinforced polymer (GFRP) composite bars have been successfully used as internal reinforcement in concrete structures given their many superior mechanical and environmental-resistance properties [16]. Examples are as reinforcement in concrete beams [17, 18], slabs [19, 20], and walls [21, 22], because their high strength and modulus of elasticity is almost similar to that of concrete. Recently, GFRP bars have also been used as reinforcement

in concrete columns [23-36]. Accordingly, concrete columns with longitudinal and transverse GFRP reinforcement under axial loads have been shown to have better performance and more stable behavior than their steel-reinforced counterparts after the concrete's peak strength has been reached. This can be attributed to the high strength and linear elastic behavior of GFRP longitudinal and transverse reinforcement, which continue to resist axial and lateral loads, respectively, until failure without any reduction in their stiffness. Very recently, a study [37] investigated comprehensively the behavior of the GFRP bars under compression, where it predicted the mode of failure and the maximum compressive strength of these bars based on the diameter and the length counting for the low modulus of elasticity of such bars. Because of this behavior, GFRP bars have the potential to overcome the brittle behavior of steel-reinforced HCCs.

This study reviews the state-of-the-art in HCCs to identify the effect of the main design parameters influencing the structural behavior of HCCs and determines the general structural issues associated with steel-reinforced HCCs. Moreover, this review study addresses the challenges affecting the durability and sustainability of the existing steel-reinforced concrete columns. In addition, the fundamental behavior of concrete columns internally reinforced with glass fiber-reinforced polymer (GFRP) bars is analyzed to explore the potential of using these materials to overcome the structural and environmental issues of steel-reinforced HCCs.

HCC BEHAVIOR AND DESIGN PARAMETERS

Comparison of steel-reinforced solid and hollow concrete columns

HCC behavior is affected by a number of design parameters. The displacement capacity and the strength after steel yielding in HCCs are generally low due to the unconfined concrete core. This can be explained by the differences in stress distribution in SCCs and HCCs. The SCC cross section subjected to axial stress (σ_{axial}) tends to expand laterally from the center to release the stored energy. The confining stress induced by the lateral reinforcement, however,

acts to prevent the SCCs from failure, initiating in-plane stress in the circumferential (σ_{circ}) and radial (σ_{rad}) directions, as shown in **Figure 1a**. In this case, the section is subjected to three types of stress (triaxial stress state). Since HCCs have no inner concrete core, lateral expansion caused by axial stress (σ_{axial}) can result in nonuniform lateral confining stress as there will be no σ_{rad} resisting the σ_{circ} in the concrete wall (**Figure 1b**). In that case, the section is subjected to biaxial stress. These internal stresses act in the cross section to provide resistance to the applied loads. The effect of triaxial and biaxial stresses becomes critical if the outer surface of the concrete section is confined to prevent lateral expansion. Otherwise, concrete crushing will occur because of the brittleness of the concrete. Based on the definition of both stress formations, triaxial stress can lead to higher confined strength values than biaxial stress due to the former's higher lateral confinement. Past research [38] found that both solid and hollow confined concrete columns showed almost the same axial strain at failure, but the SCCs had lateral expansion 4 times greater than the HCCs (**Figure 2a**). It should be mentioned that this ratio is limited to this experimental study but the behavior behind that is due to the discontinuity in the radial stress inside the concrete core of the HCCs owing to the hollowness. Liang and Sritharan [39] explained that the lateral expansion of concrete increases as the concrete wall thickness increases and converges on that of SCCs (see **Figure 2b**). This means that, unless SCCs have high lateral stiffness to confine the concrete, high axial-deformation capacity cannot be achieved and early failure can be expected. On the other hand, the concrete wall of the HCC has to be thick enough (at least 10% of the outer diameter) to prevent the concrete from failing in shear [8, 40].

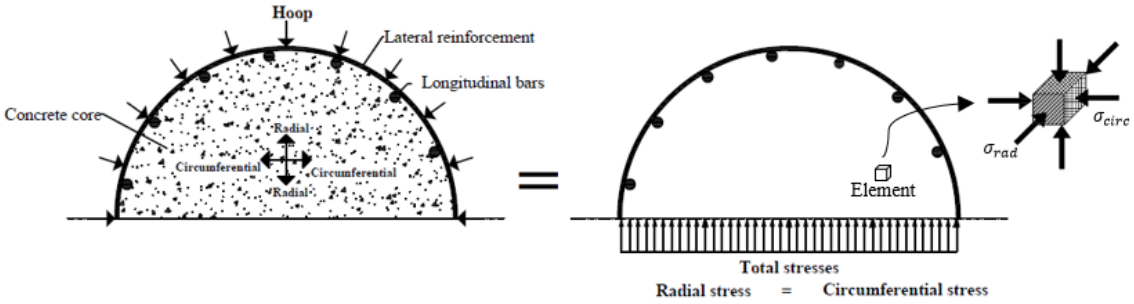

(a) SCC

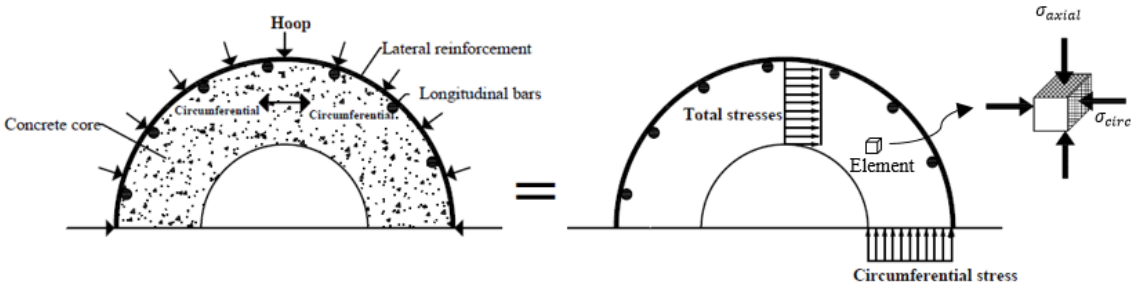

(b) HCC

Figure 1. Stress formation within the concrete core of SCC and HCC

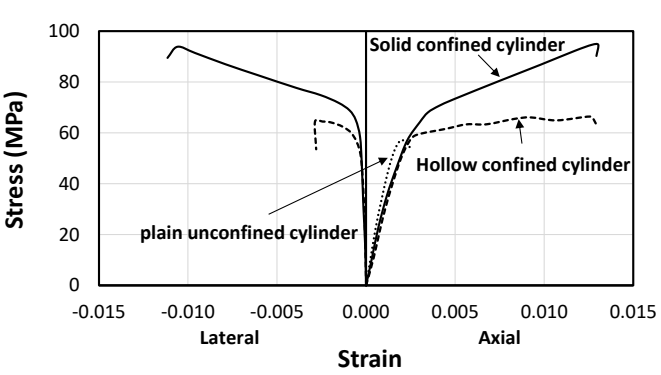

(a) Stress–strain behavior [38]

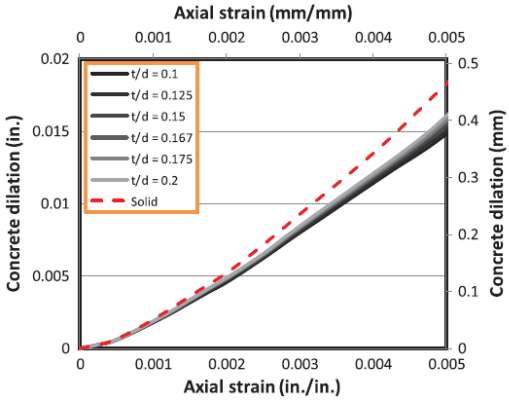

(b) Lateral concrete dilation [39]

Figure 2. Behavioral comparison of HCCs and SCCs

Experimental investigations on steel-reinforced HCCs

A comprehensive review of the experimental works on HCCs was conducted and is summarized in **Table 1**. The review was limited to HCCs with steel reinforcement or plain concrete without inner confinement of the concrete core. **Table 1** presents the studies by publication year and loading conditions. The detailed design parameters for the experimental

samples are then reported such as the axial-load ratio ($\frac{P_o}{f_c' A_c}$) (the ratio between the applied axial load to the maximum axial load capacity), geometry of the cross section (*G*), height of samples (*H*), the outer diameter of the circular section (o) or the outer dimensions of the square and rectangular sections (*OD*), the inner diameter of the circular section (*i*) or the outer dimensions of the square and rectangular sections (*ID*), the inner-to-outer diameter (i/o) ratio, reinforcement ratio (ρ), number of longitudinal reinforcement bars (N_L), presence of cross ties (*CT*), volumetric ratio (ρ_v), concrete compressive strength (f_c'), circular column (*C*), square column (*S*), rectangular column (*R*), yes (*Y*), no (*N*), both (*B*), and the design parameters of the experimental study.

Table 1. Review of past experimental studies conducted on HCCs

Study number	Author	Year	Loading Type	$\frac{P_o}{f'_c A_c}$	G	H (mm)	(o) or OD (mm)	(i) or ID (mm)	i/o ratio	ρ (%)	N_L	CT	ρ_v (%)	f'_c (MPa)	Design Parameter
1	Mander [3]	1983	Hysteretic	0.1 0.3 0.6	S	3200	750×750	510×510	0.68	1.55	2	Y	1.72,1.29, 0.86	30.0	$\frac{P_o}{f'_c A_c}$, ρ_v
2	Zhan [4]	1986	Hysteretic	0.05-0.28	C	1600	400	212 250 290	0.53 0.63 0.73	2.56	1	-	1.13-1.36	29.6	$\frac{P_o}{f'_c A_c}$, ρ_v, i/o ratio
3	Whittaker [5]	1987	Hysteretic	0.125 0.3	C	3150	800	600 700	0.75 0.88	2.29 2.88	2	Y	1.38-2.37	35.0	$\frac{P_o}{f'_c A_c}$, ρ_v, ρ, i/o ratio
4	Kishida et al. [41]	1998	Hysteretic	-	C	900	300	180 225	0.60 0.75	1.41 1.66	1	-		93.5	$\frac{P_o}{f'_c A_c}$, ρ_v, ρ, i/o ratio
5	Osada et al. [11]	1999	Hysteretic	0.040	C	1800	350	150	0.43	3.4	1	-	0.14	23.5 45.0	f'_c, $wrapping$
6	Hoshikuma and Priestely [7]	2000	Hysteretic	0.13	C	3480	1524	1244	0.82	1.45 3.18	1	-	0.71	38.0	ρ
7	Ranzo and Priestely [8]	2001	Hysteretic	0.05 0.15	C	3880	1560 1524	152 139	0.81 0.82	1.34 2.25	1	-	0.35	35.0	$\frac{P_o}{f'_c A_c}$, ρ
8	Fam and Rizkalla [38]	2001	Axial	Full	C	336	219	95 133	0.49 0.68	N/A	1	-	8.96 6.40	58.0	i/o ratio, $wrapping$
9	Yeh et al. [9]	2001	Hysteretic	0.10	C	5500 3500	1500	900	0.60	2.15	2	Y	0.28-0.625 0.185	32.1	ρ_v
10	Yeh et al. [10]	2002	Hysteretic	0.082-0.176	S	6500 4500 1800	1500×1500 500×500	900×900 260×260	0.60 0.52	1.7 1.9	2	Y	0.01-0.032	32.3	$\frac{P_o}{f'_c A_c}$, ρ_v
11	Mo and Nien [42]	2002	Hysteretic	0.054-0.132	S	1800 1500	500×500	260×260	0.52	2.07	2	Y	0.44- 1.36	58.7	$\frac{P_o}{f'_c A_c}$, ρ_v, AR
12	Mo et al. [12]	2003	Hysteretic	0.06 0.19	S	2000	500×500	300×300	0.60	1.13	2	Y	0.49-0.98	24.6-49.9	$\frac{P_o}{f'_c A_c}$, ρ_v, f'_c
13	Pinto et al. [13]	2003	Hysteretic	0.09	R	5750 13250	2740×1020	2320×680	0.72	0.4	2	N	0.09	38.9 51.6	AR
14	Pavese et al. [14]	2004	Hysteretic	0.06 0.19	S	900 1350	450×450	300×300	0.67	1.07 1.76	2	Y	0.13 0.25	33.0	$\frac{P_o}{f'_c A_c}$, AR, $wrapping$
15	Calvi et al. [43]	2005	Hysteretic	0.06-0.21	S	900 1350	450×450	300×300	0.67	1.07 1.76	2	N	0.13 0.25	32.5	$\frac{P_o}{f'_c A_c}$, AR

16	Modarelli et al. [44] and Micelli and Modarelli [45]	2005, 2013	Axial	1.0	C	300	150	50	0.33	-	-	-	-	28.0 38.0	f_c', G, $wrapping$
						500	250	150	0.60						
					S	300	150×150	50×50	0.33						
					R	400	200×150	100×50	0.41						
						600	300×150	200×50	0.47						
17	Yeh and Mo [46]	2005	Hysteretic	0.08- 0.19	C	3500	1500	900	0.60	1.69	2	Y	0.64	18.0	$\frac{P_o}{f_c'A_c}$, f_c', $wrapping$
					S		1500×1500	900×900	0.60	2.15			0.71	31.0	
18	Lignola et al. [1]	2007	Axial	1.0	S	3020	360×360	240×240	0.67	1.75	1	-	0.26	32.0	$Wrapping$
19	Delgado et al. [47]	2008	Hysteretic	0.063	S	1600	450×450	300×300	0.67	1.79	1	-	0.075	35.0	$G, wrapping$
				0.070	R		900×450	750×300	0.75						
20	Turmo et al. [48]	2009	Shear	0	C	3000	600	400	0.67	2.4	1	-	0.15	24.7 32.2	f_c'
21	Kusumawardaningsih and Hadi [2]	2010	Axial	1.0	C	925	205	69	0.34	2.32	1	-	2.95	72.0	$G, wrapping$
					S		182×182	61×61	0.33	1.77			2.38		
22	Lignola et al. [49]	2011	Axial	1.0	R	3050	737×508	509×280	0.62	1.7	1	-	0.29	44.7	$Wrapping$
23	Yazici [50]	2012	Axial	1.0	C	500 885	150	56	0.37	3.5	1	-	2.41	76.5	$AR, wrapping$
24	Kim et al. [51]	2012	Monotonic lateral and pure cyclic	0	R	900- 1800	900×600	540×400 640×340 740×440	0.63 0.63 0.78	1.8 2.7	1	-	0	24.6	ρ, i/o ratio, AR
25	Cheon et al. [52]	2012	Hysteretic	0.065- 0.15	C	3500	1000	500 750	0.50 0.75	0.83- 2.00	1	-	0.60 1.20	32.5	$\frac{P_o}{f_c'A_c}$, ρ_v, ρ, i/o ratio
26	Kim et al. [53]	2013	Axial	1.0	C	1000	1990	1590	0.80	1.2	2	Y	0.36	27.0	ρ_v, G
					R	600	540×150*	-	-	1.8			0.84	21.0	
27	Han et al. [54]	2013	Hysteretic	0.1 0.2	R	1400	550×360	260×120	0.42	1.4 2.1	2	Y	2.50 3.50	42.6	$\frac{P_o}{f_c'A_c}$, ρ_v, ρ
28	Zhang et al. [55]	2013	Hysteretic	0.1	R	1240	500×360	300×160	0.52	1.40	1	-	0.72	38.7 43.8	f_c'
29	Shin et al. [56]	2013	Monotonic lateral and pure cyclic	0	R	1200	900×600	640×340	0.63	1.8	1	-	0	24.6 39.4 47.4	f_c'
30	Hadi and Le [57]	2014	Axial	1.0	S	800	200×200	80×80	0.40	1.35	1	-	0.94	40.0	$Wrapping$
31	Han et al. [58]	2014	Hysteretic	0.2	R	1400 2800	550×350	330×130	0.47	1.05	2	Y	0.49	30.4	$AR, wrapping$
32	Volgyi et al. [59]	2014	Shear and flexure	0	C	3000	300	55 90	0.18 0.30	1.92- 2.56	1	-	0.21-0.46	60.0 75.0	ρ, i/o ratio, ρ_v, f_c'
33	Kim et al. [60]	2014	Hysteretic	0.1	C	4900	1400	1000	0.71	1.30- 1.53	2	Y	0.09-1.0	22.0	ρ_v, ρ, G
					S		1000×1000	500×500	0.50						
34	Liang at al. [15]	2015	Hysteretic	0.03- 0.20	C	1200	300	200 250	0.67 0.83	1.56	1	-	1.80	46.8	$\frac{P_o}{f_c'A_c}$, i/o ratio, G
					S		300×300	200×200 240×240	0.67 0.80	1.47			1.84		

35	Lee et al. [6]	2015	Hysteretic	0.065-0.15	C	4000	1000	500 750	0.5 0.75	0.83-2.00	1	-	0.69 1.38	32.5	$\frac{P_o}{f_c' A_c}$, ρ_v, ρ, i/o ratio
				0.08 0.125		5400	1400	980	0.7	1.0 2.0	2	B	0.19-0.38	27.5 39.0	
36	Prado et al. [61]	2016	Hysteretic	0.06	R	4500	1200×800	150	0.68	2.79	2	Y	0.01-0.02	26.9	ρ_v
37	Cassese et al. [62]	2017	Hysteretic	0.05	R	900 1500	600×400	400×200	0.58	0.88	1	-	0.12	17.0	AR
38	Jameel et al. [63]	2017	Axial	1.0	C S	300	106×106	35×35	0.33	-	-	-	-	45.0	G
39	Hadi et al. [64]	2017	Axial	1.0	C	800	212	50×50	0.27	1.28	1	-	2.00	47.0	G
					S	800	150×150		0.33	2.26					
40	Cassese et al. [65]	2018	Hysteretic	0.05	C	1100 1650	550	350	0.64	0.85	1	-	0.06	15.6	AR
41	Irawan et al. [66]	2018	Hysteretic	0.08 0.16	C	3500	400	200	0.50	0.32	1	-	0.16	54.4 67.5	$\frac{P_o}{f_c' A_c}$, f_c'

A statistical study was conducted on the information presented in **Table 1** to illustrate the cumulative percentage of the experimental studies on HCCs published from 1983 to 2018 (**Figure 3**). **Figure 3** shows that research focusing on HCCs has significantly increased in the last two decades, underscoring the structural importance and effectiveness of such systems for structural columns. These experimental studies can be divided into four regions. Period A (1983–1997) consists of the first attempts at investigating HCCs by identifying their behavior and capacity according to some design parameters such as axial-load ratio ($\frac{P_o}{f_c' A_c}$), i/o ratio, and volumetric ratio (ρ_v). Period B (1998–2005) witnessed a significant increase in the number of experimental studies exploring the effect of other design parameters—such as reinforcement ratio (ρ), geometry (G), and aspect ratio (AR)—to gain a greater understanding of HCC behavior. Experimental studies in Period C (2006–2011) included the incorporation of new techniques to improve HCC behavior, such as wrapping the column with carbon-fiber sheets. Significant field testing began after 2012 (Period D), exploring with new approaches and techniques such as changing the lateral-reinforcement configuration and increasing the reinforcement ratio by providing double layers of longitudinal reinforcement. Inserting double skin (outer and inner) tubes and externally wrapping with composite materials were also attempted. For a review and discussion of these techniques, see Al-Saadi et al. [67] and Han et al. [68].

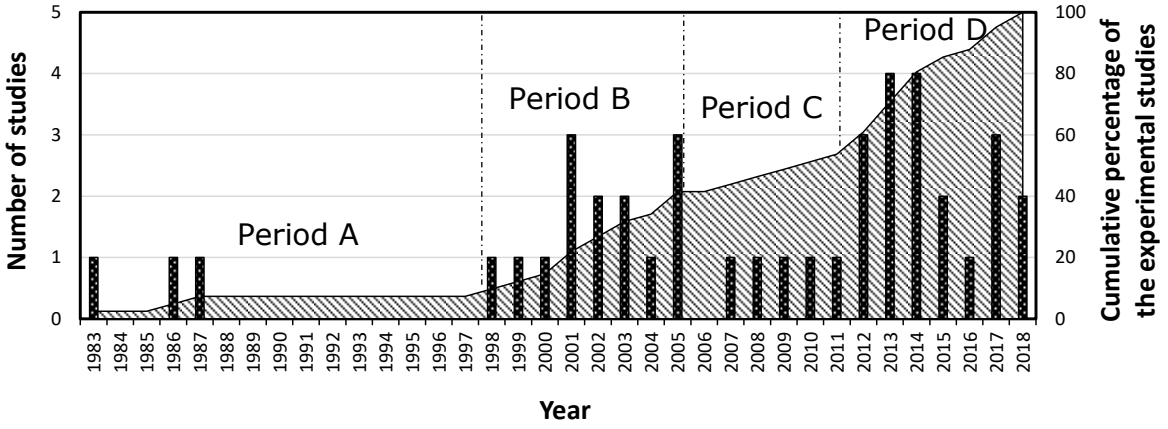

Figure 3. Cumulative percentages of the experimental studies on HCCs from 1983 to 2018

As presented in **Figure 4**, most of the studies (63%) adopted the hysteretic type of loading to investigate HCC behavior. This type of loading has been primarily adopted for HCCs because axial and lateral cyclic loads are the loading requirements for designing bridge piers. The second-most frequent loading type investigated (24%) focused on HCC axial behavior. This is because as it was found that the axial-load ratio applied during hysteretic load tests significantly affected HCC overall behavior. Cyclic and monotonic lateral loading, bending, and shear accounted for 7%, 3%, and 3%, respectively, of the total experimental studies. They were investigated as they are the loading conditions that HCCs are subjected to when used as slender columns and electric poles.

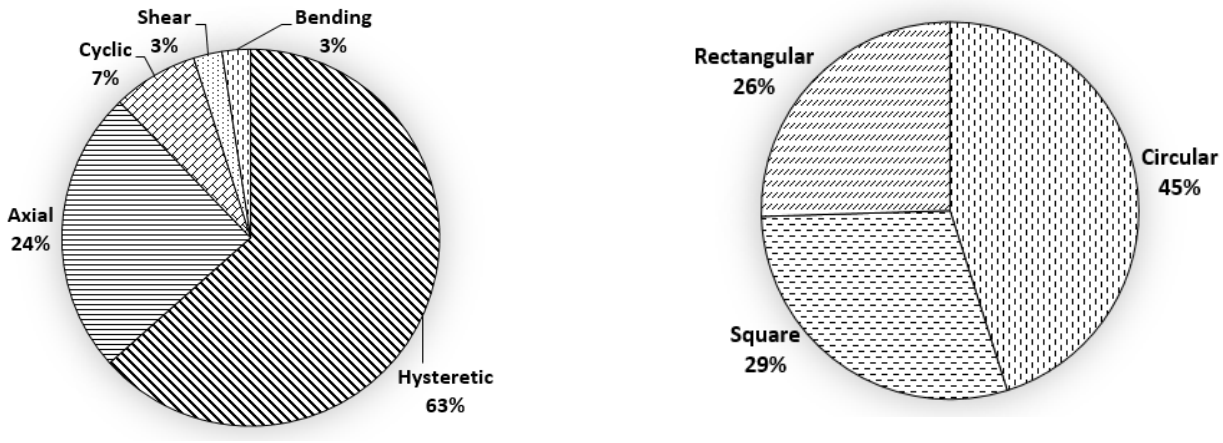

(a) Loading type (b) Column geometry

Figure 4. Distribution of studies on HCCs based on loading conditions and geometric configurations

Geometry is another important factor in HCC design as it affects the stress distribution within the column cross section. Square and rectangular sections create a nonuniform stress state, leading to localized stress concentration, whereas circular sections provide uniform stress within the column [3]. Correspondingly, most of the HCCs investigated had circular cross sections (45% of the total cross sections tested), as shown in **Figure 4.b**. To evaluate the effectiveness of HCCs in concrete bridge piers, Mander [3], Yeh et al. [9], and Mo et al. [12, 42] investigated square HCCs. For the same reason, Pinto et al. [13], Delgado et al. [47], and

Kim et al. [51] investigated rectangular HCCs to increase HCC rigidity in the main loading direction. Out of the published studies on HCCs, 29.0% involved square sections, compared to 26.0% with rectangular cross sections.

Critical design parameters affecting overall HCC behavior were also analyzed (see **Figure 5**). As most HCCs were tested under hysteretic loads, the axial-load ratio ($\frac{P_o}{f_c' A_c}$) would be expected to be the parameter most studied, as this represents the applied load under combined axial and lateral cyclic loading. Studies involving this parameter comprised 21.6% of the total number of studies. It should be mentioned that the axial load in some studies that adopted hysteretic loading [41, 66] was achieved by adding prestressed reinforcement instead of an externally applied axial load. The second-most investigated parameter was volumetric ratio (ρ_v) (20.3% of the total number of studies). This design parameter was investigated either by increasing the diameter of the steel ligatures or decreasing the spacing between them. Some studies manipulated the arrangements of the lateral reinforcement [12, 53] by tying together two layers of longitudinal reinforcement [9, 10, 12, 42, 51, 53]. A number of experimental studies were implemented to increase HCC stiffness and compensate for the absence of an inner concrete core by increasing the reinforcement ratio (ρ). Increasing ρ can be achieved by either increasing the diameter or the number of longitudinal bars. Studies on this parameter comprise 13.3% of the total studies reported in **Table 1**. Studies have shown that HCCs have to have adequately thick wall to prevent premature shear failure and minimize compression failure in the concrete core. Therefore, the effect of the i/o ratio was studied in 12.0% of the total reported studies. Other design parameters investigated were f_c', aspect ratio, and geometry, comprising 12.0%, 10.7%, and 10.7%, respectively, of the total reported studies.

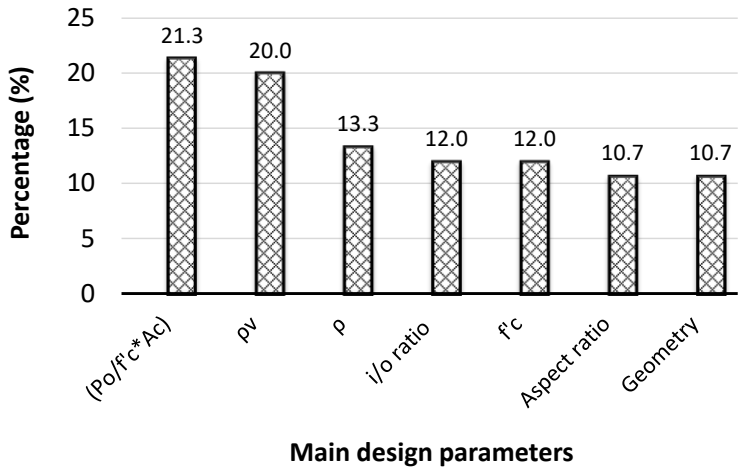

Figure 5. Critical design parameters for HCCs

Influence of the critical design parameters on HCCs

The critical design parameters based on the priority in **Figure 5** (ρ_v, ρ, *i/o*, and f_c') were analyzed in detail to evaluate their effects on HCC behavior. The ($\frac{P_o}{f_c' A_c}$) ratio was taken as equal to 1.0 (full axial load) to eliminate the contribution of the lateral load and the effect of this loading on the behavior of the HCC system. It should be noted that the HCC samples tested under the hysteretic-loading condition were adopted only at maximum lateral displacement as this results in the ultimate compressive stress in the inner concrete wall.

Inner-to-outer diameter (i/o) ratio

Increasing the i/o ratio reduces the amount of material used and increases the effect of biaxial stress in the cross section of HCCs. The increase in i/o ratio decreases the thickness of the inner concrete core, which leads to brittle failure, driven mostly by the shear of the concrete after it reaches its ultimate compressive strength capacity. Referring to **Table 1**, nine studies considered the i/o ratio as a design parameter: five subjected their samples to hysteretic loading; one to cyclic and monotonic lateral load; one to concentric compression; and one to shear loading.

Table 2 gives the influence of the i/o ratio under hysteretic load on the ductility, load capacity, and failure mode. The ductility (Δ_u/Δ_y) ratio in the table is the ratio of the ultimate displacement (Δ_u) corresponding to 80% of the maximum load after peak strength to the displacement corresponding to the yielding of the steel bars (Δ_y); the mode of failure is categorized as flexural (F), concrete-core crushing (C), shear (S), or a combination. Accordingly, the higher i/o ratio resulted in failure that was less ductile and in lower lateral load capacity than HCCs with low i/o ratios. This parameter is, however, also affected by other design parameters such as ($\frac{P_o}{f_c' A_c}$) ratio, ρ_v, ρ, and f_c'. These findings can be seen in the change in failure mode when the higher i/o ratio (thickness reduction of the inner concrete core) led to concrete-core crushing or shear failure (see **Table 2**). There is an inverse relationship between the thickness of the concrete wall and the concrete core achieving its ultimate compressive strength. Therefore, it can be concluded from **Table 2** that failure was governed by flexure in the HCCs with adequately thick concrete cores (i/o ratios of up to 0.6). At higher i/o ratios (0.6 to 0.8), the mode of failure shifted from flexural to concrete-wall crushing due to the lower capacity of the thin core to resist the applied load. Shear failure will always occur in HCCs with i/o ratios of more than 0.8 when high amounts of lateral reinforcement (ρ_v) is provided. Conversely, the failure would occur as concrete-core crushing. Furthermore, Zahn [4] reported the mechanism of the HCCs under eccentric and flexural loads by that the increase in the concrete wall thickness in HCC resulting in a closer neutral axis to the inner unconfined concrete wall which leads to reduce the longitudinal strain at that part of concrete and shows flexural failure behavior compared to the thinner walled HCC that showed concrete crushing.

Table 2. Effect of i/o ratio on ductility and load capacity

Study Number	Authors	i/o ratio	Δ_u/Δ_y	Load Capacity (kN)	Mode of Failure
2	Zahn [4]	0.53	12.4	225	F

3	Whittaker [5]	0.63	5.2	221	F-C
		0.73	4.6	211	F-C
		0.75	12.0	440	F-C
		0.88	2.5	260	C
4	Kishida et al. [11]	0.60	5.5	370	F
		0.75	3.4	325	C
24	Kim et al. [51]	0.63	1.9	522	F-S
		0.78	1.6	337	S
25	Cheon et al. [52]	0.50	7.4	642	F
		0.75	3.7	596	F-C
34 & 35	Liang et al. [15] and Lee et al. [6]	0.67	5.2	70	F
		0.83	1.9	38	S

Micelli and Modarelli [45] tested hollow plain-concrete columns with i/o ratios of 0.33 and 0.60 under pure concentric load, as detailed in **Table 1**. They found an insignificant reduction (within the standard deviation of f_c') in the axial strength for columns with an i/o ratio of 0.33 compared to the solid columns. A 60% reduction in axial strength was, however, observed in the columns with an i/o ratio of 0.60 due to the shear effect, which led to the premature failure of the thinner concrete wall. In the same experiment, hollow plain-concrete columns with i/o ratios of 0.33 and 0.60 confined externally with fully wrapped CFRP sheets were tested. The stress–strain relationship (see **Figure 6a**) shows that the increase in i/o ratio from 0.33 to 0.60 increased the strength and strain by 51% and 13%, respectively. Fam and Rizkalla [38] used the same test setup by fully wrapping two hollow plain-concrete columns with i/o ratios of 0.49 and 0.68 with CFRP sheets. The stress–deformation behavior in **Figure 6b** shows that 10% and 18% enhancement in the strength and deformation, respectively, were achieved by reducing the i/o ratio from 0.68 to 0.49.

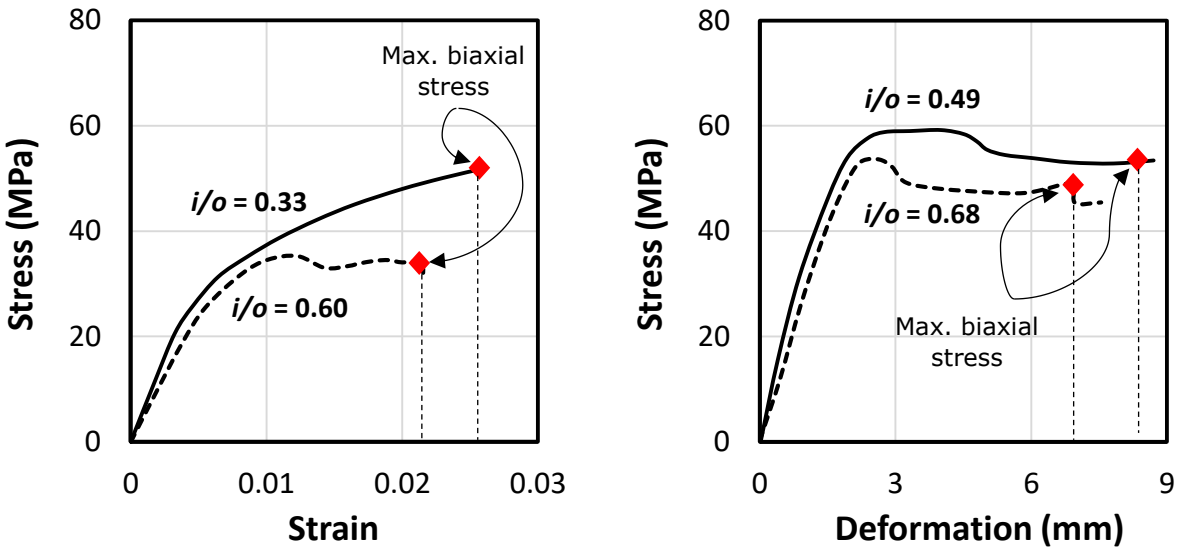

(a) Column from [45] (b) Column from [38]

Figure 6. Stress–strain and deformation of fully wrapped HCCs with different *i/o* ratios

Reinforcement ratio and longitudinal-bar arrangement

Table 1 provides data from 10 studies that evaluated the effect of reinforcement ratio (ρ) on HCC behavior: eight used hysteretic loading; one monotonic lateral loading; and another bending. The main aim of increasing ρ was to increase the strength and compensate for the reduction in stiffness of HCCs due to the lack of concrete core. The increase in ρ was achieved by increasing the diameter [7, 8, 54] or the number [6, 13] of the longitudinal bars. **Table 3** summarizes the effect of increasing ρ on the load capacity and ductility of the HCCs. Note that the load capacity was normalized in **Table 3** by dividing the higher on the lower load capacity of the columns tested by each researcher. The test results in **Figure 7a** show that the higher ρ increased the load capacity of the HCCs. **Figure 7b** also shows a reduction in ductility as a result of increasing ρ due to the severe compression crushing in the inner concrete wall. It should be mentioned that increasing ρ by increasing the number of bars yielded less reduction in ductility than increasing the bar diameter, owing to the increased lateral confinement as more bars were covering the unconfined concrete-core area. Han et al. [54] and Lee et al. [6] also observed this behavior. When the longitudinal bars yielded, the high axial load resisted by the

steel reinforcement was directly transferred to the concrete wall, overstressing and crushing the concrete. This mechanism is due to the fact that steel reinforcement significantly losing its stiffness after reaching its yield strain while the concrete is still resisting due to has higher ultimate compressive strain until reaching its peak strength where it starts to fail by crushing.

Table 3. Effect of ρ on ductility and load capacity

Study Number	Authors	ρ (%)		Δ_u/Δ_y		Load Capacity (kN)		Normalized Load Capacity
6	Hoshikuma and Priestley [7]	1.45	3.18	4.83	2.34	730	1150	1.58
7	Ranzo and Priestley [8]	1.34	2.25	7.85	4.17	1150	1350	1.17
14	Pavese et al. [14]	1.07	1.76	7.17	3.25	220	245	1.11
27	Han et al. [54]	1.40	2.10	5.40	5.20	195	146	1.07
35	Lee et al. [6]	1.17	2.00	4.60	3.70	421	596	1.41

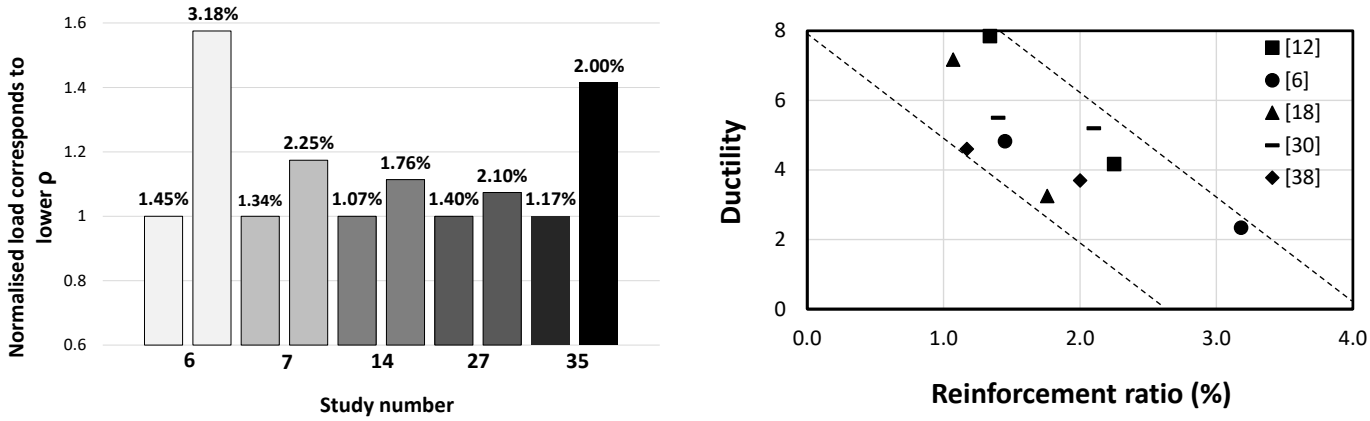

(a) Strength (b) Ductility

Figure 7. Effect of ρ on HCC strength and ductility

Several authors [6, 9, 12, 60] changed the arrangement of the longitudinal reinforcement to overcome the brittle failure behavior of HCCs. They reinforced HCCs with two layers of steel bars: one near the outer face and one near the inner face. This approach significantly enhanced the strength and ductility of the HCCs due to the higher confinement efficiency compared to columns with a single layer of longitudinal steel bars, especially when cross ties (CTs) between

the two reinforcing layers were provided [6, 53]. This kind of design, however, requires more reinforcing materials and increases construction costs.

Volumetric ratio (ρ_v) and spacing between lateral reinforcement

The parameter of volumetric ratio and spacing between lateral reinforcement was the second-most frequently investigated parameter for HCCs (a total of 15 studies). The purpose was to address the limited ductility exhibited by HCCs with low lateral confinement. Thirteen of the 15 studies tested HCCs under hysteretic loading; one under axial loading; and one under flexural loading. It is worthy mentioned that the mechanism of providing high volumetric ratio beings in increasing the resistance of the lateral reinforcement by confining the concrete core to delay the failure and/or increase the axial strength capacity in advance of the characterized strength. Mander [3] varied the ρ_v, finding that the HCCs behaved in a ductile manner similar to that of solid columns at high ρ_v levels. He also suggested that the increase in ρ_v can be achieved by reducing the spacing between lateral reinforcement or increasing its diameter. Lignola et al. [49] reported that the wide spacing between ligatures resulted in premature HCC failure due to compression crushing of the concrete wall and buckling in the longitudinal reinforcement. **Table 4** summarizes the test results from the literature showing the effect of ρ_v on ductility and load-carrying capacity of the HCCs. As shown in **Figure 8**, the increase in ρ_v generally increased the ductility. The increase in ρ_v by increasing the spacing of the lateral reinforcement [3, 9, 10] was found to yield higher ductility than did increasing the diameter of the lateral reinforcement [42, 60]. This is because reducing the spacing of the lateral reinforcement confined the concrete while increasing the crushing strength of the concrete core and the buckling strength of the longitudinal bars. On the other hand, increasing ρ_v slightly affected the load-carrying capacity. Increasing the lateral confinement yielded no more than an 11% increase in column capacity, except in one study [54] in which the columns were subjected to bilateral instead of unilateral cyclic load.

Table 4. Effect of ρ_v on ductility and load capacity

Study Number	Authors	ρ_v (%)		Δ_u/Δ_y		Load Capacity (kN)		Normalized Load Capacity
1	Mander [3]	2.08	3.12	5.92	8.15	415	418	1.01
3	Whittaker [5]	1.97	2.37	4.07	5.04	270	299	1.11
9	Yeh et al. [9]	2.80	6.30	2.80	9.00	1431	1581	1.10
10	Yeh et al. [10]	1.50	3.20	3.45	5.54	2610	2840	1.09
11	Mo and Nien [42]	0.76	1.36	3.90	4.30	350	360	1.03
25	Cheon et al. [52]	0.60	1.20	6.00	7.40	431	442	1.03
27	Han et al. [54]	2.50	3.50	3.70	5.20	195	146	0.75
33	Kim et al. [60]	0.86	1.94	6.10	6.30	785	800	1.02

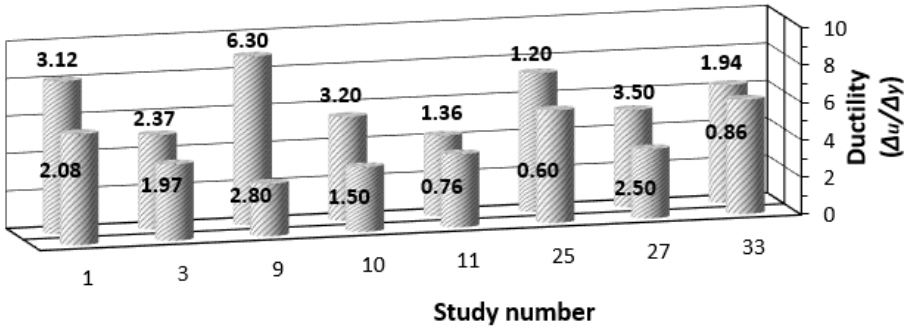

Figure 8. Effect of increasing ρ_v on HCC ductility

Some studies compared the behavior of the HCCs with and without external CFRP wrapping [2, 14, 47, 49, 50, 57, 58, 64] (denoted in **Table 1** as wrapping). Kusumawardaningsih and Hadi [2] fully wrapped the outer surface of steel-reinforced HCCs with CFRP sheets. They found that the fully wrapped columns exhibited deformation capacity and strength more than 100% and 50% higher, respectively, than the unwrapped columns (**Figure 9a**). Yazici [50] observed the same enhancement, as shown in **Figure 9b**, when the deformation was six times higher and the strength enhanced by more than 80% after wrapping steel-reinforced HCCs with CFRP sheets. This significant enhancement in strength and ductility might be due HCCs having lower lateral expansion than SCCs. This would allow them to resist higher stresses and exhibit more deformation before failure. Fam and Rizkalla [38] also observed that the inner face of the hollow concrete underwent tension until reaching the elastic peak strength due to the concrete

wall's lateral expansion. Afterwards, inward expansion of the HCC inner face was observed when the stress in the concrete shifted from tension to compression. This means that the section increased in area, which resulted in increased deformations and load capacity.

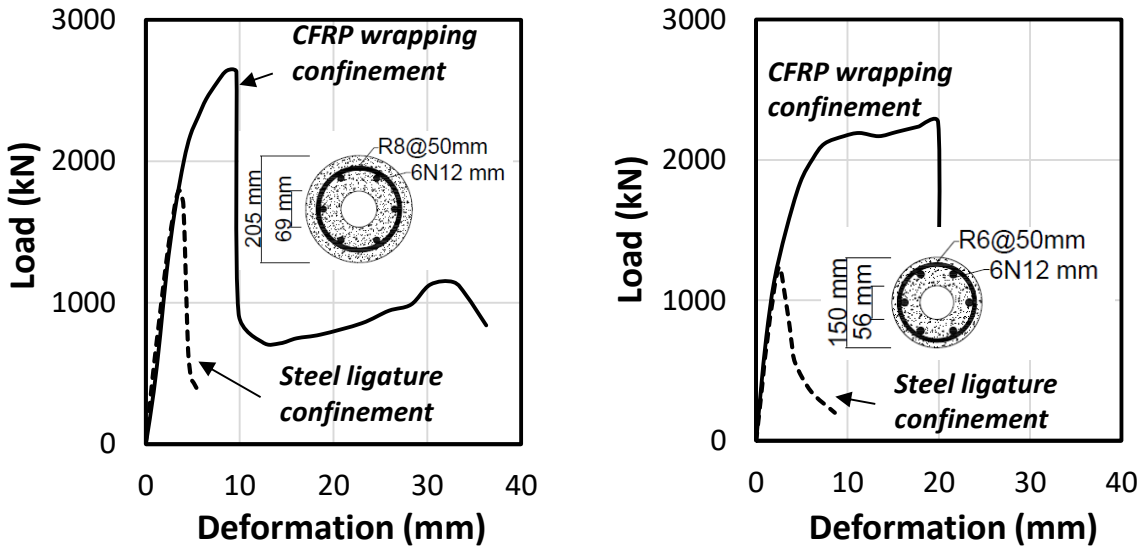

(a) Study [2] (b) Study [50]

Figure 9. Effect of providing full confinement to HCCs with CFRP-sheet wrapping [2, 50]

Concrete compressive strength

Concrete compressive strength (f_c') plays a major role in the overall behavior of HCCs. Increasing f_c' increases the brittle behavior of the concrete due to the reduction in the Poisson's ratio effect [12, 69, 70]. This design parameter has been examined nine times, as listed in **Table 1**. Of these studies, five using different f_c' in HCCs were conducted under hysteretic loading: two under bending and shear loading; one under monotonic lateral loading; and one under concentric compression loading. Mo et al. [12] tested square HCCs under hysteretic loading with different f_c' and observed that the column with a higher f_c' experienced more ductile failure behavior and energy dissipation than the column with a lower f_c', as shown in **Figure 10a**. The more ductile behavior of HCCs with higher f_c' is due to column failure caused by the rupturing of the steel bars with the concrete still intact during cyclic loading. Columns with lower f_c' could not adequately distribute the shear stress caused by the combined axial and

lateral loading. This caused in an abrupt drop in strength and produced very large inclined shear cracks, leading to buckling of the longitudinal bars. These findings are supported by Osada et al. [11], who noted higher ductility and lateral-load resistance in HCCs with higher f_c'. In contrast, the testing of well-confined HCCs made with plain concrete at different f_c' subjected to pure concentric load [45] showed that the columns with higher f_c' (38 MPa) had 44% less deformation and 27% lower confinement effectiveness (σ_{max}/f_c') than the columns with lower f_c' (28 MPa), as shown in **Figure 10b**. The σ_{max} is the maximum confined stress in the cross-section area at the plastic stage (denoted by the solid circles in **Figure 10b**). This behavior was due to the higher Poisson's ratio of concrete with a lower f_c', which led to a better distribution of lateral stresses and higher axial deformation [69]. Another method of increasing f_c' is to increase the concrete's tensile-strength capacity, as did Zhang et al. [55] and Shin et al. [56], by adding steel fibers to the concrete. They found that using steel fibers significantly increased the strength, ductility, and energy dissipation of the HCCs, allowing the columns to exhibit higher cyclic capacity and lower strength loss by limiting the growth of shear cracks and facilitating flexural failure compared to the columns without steel fibers.

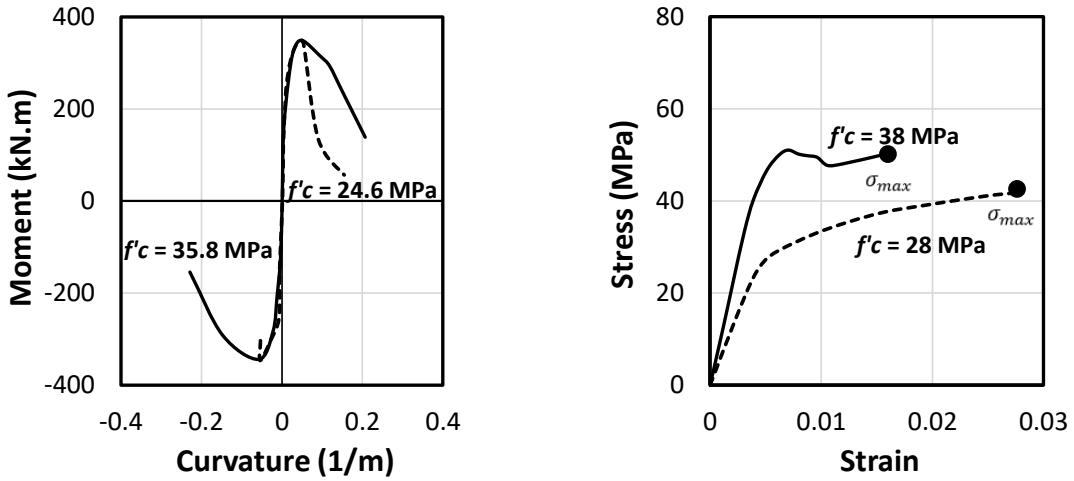

(a) [12] (b) [45]

Figure 10. Effect of f_c' on the (a) hysteretic and (b) axial behaviors of HCCs

Slenderness and geometry

Figure 5 shows that aspect ratio (AR) and geometry (G) were the least investigated design parameters for HCCs with a total of eight studies for each parameter. Aspect ratio (AR) is the ratio between the distance from the location of the load to the column base and the dimension of the column in the direction of loading. **Table 5** summarizes the studies that considered AR as a design parameter. The results indicate that an increase in AR shifted the failure mode from shear (in the concrete) to flexure (in the reinforcement). This is due to better energy dissipation with a more progressive failure compared to the sudden failure observed in columns with low AR. The lateral-force capacity of the shorter columns was higher than the slender ones, although the amount of resisted bending moments were almost same or slightly more for the slender columns by considering the different lever arms. Moreover, flexural failure can be expected for columns subjected to hysteretic or cyclic loads at AR greater than 2 (**Figure 11**).

Table 5. Effect of AR on ductility, moment capacity, and failure mode

Study Number	**Authors**	**Load Arm (m)**		***AR***		Δ_u/Δ_y		**Load Capacity (kN)**		**Moment (kN.m)**	
11	Mo and Nien [42]	1.50	1.80	3.00	3.60	4.40	4.50	364	332	546	598
13	Pinto et al. [13]	5.75	13.25	2.10	4.84	10.30	4.90	1300	800	7475	10600
14-15	Pavese et al. [14] & Calvi et al. [43]	0.90	1.35	2.00	3.00	6.30	8.20	217	217	195	293
24	Kim et al. [51]	0.90	1.80	1.00	2.00	-	-	525	259	473	466
31	Han et al. [58]	1.40	2.80	2.55	5.09	8.60	6.72	163	77	228	216
37	Cassese et al. [62]	0.90	1.50	1.50	2.50	1.35	3.80	278	168	250	252
40	Cassese et al. [65]	1.10	1.65	2.00	3.00	5.70	10.60	167	108	184	178

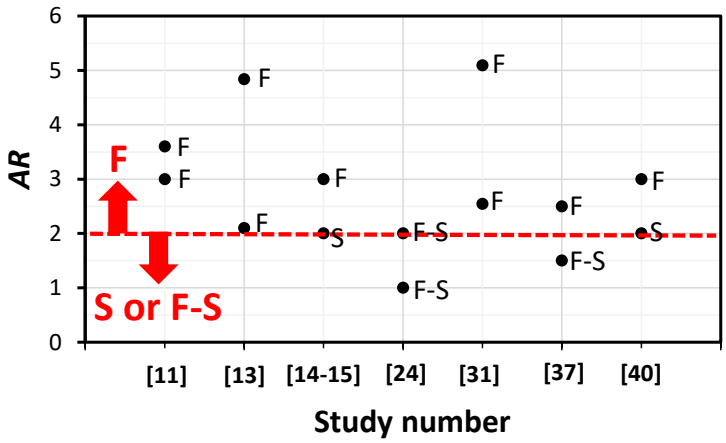

Figure 11. Effect of the aspect ratio on the failure mode of HCCs

The effect of geometry on HCC behavior has been studied by eight researchers, as listed in **Table 1**. Their studies all indicated that the circular columns had more uniform internal stress distribution than the square or rectangular columns due to the better confinement of the concrete core, which led to higher strength (**Figure 12a**). This behavior is due to the stress concentration at the corners of square and rectangular columns, causing uneven confined stress within the concrete wall. Some attempts to round the corners of square concrete columns were implemented to reduce the stress concentration [63, 64] and to enhance the behavior and confined strength of these columns (**Figure 12b**).

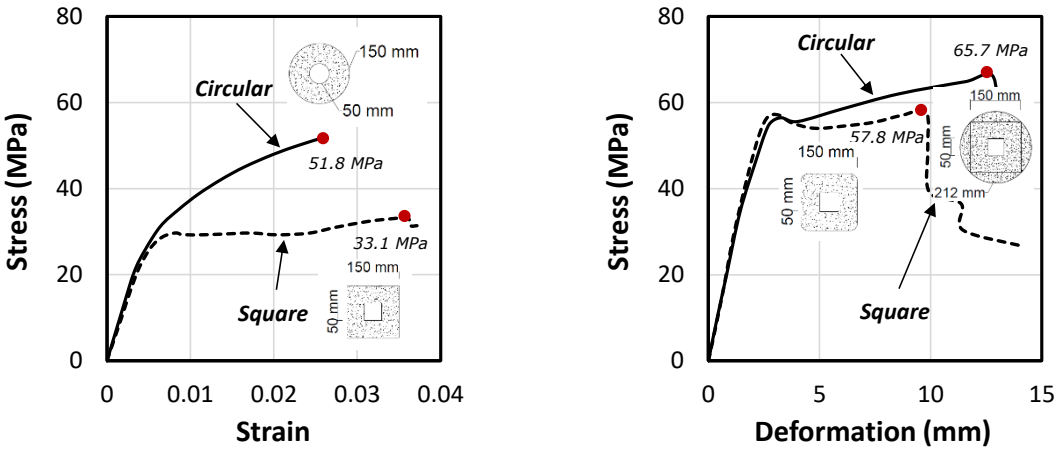

(a) Micelli and Modarelli [45] (b) Hadi et al. [64]

Figure 12. Effect of geometry on HCC behavior

Challenges in the design of steel-reinforced HCCs

The preceding sections highlight that, overall, steel-reinforced HCCs behave significantly differently than SCCs due to the absence of the concrete core, which changes the inner stress formation from triaxial in SCCs to biaxial in HCCs. Moreover, the capacity of HCCs can be comparable to or even exceed that of SCCs when appropriate levels of design parameters ((i/o) ratio, ρ, ρ_v, f_c', AR, G) are achieved. The limited ductility due to the compression failure of the inner concrete core is a significant concern in designing HCCs using steel bars. Similarly, steel corrosion has become a problem in concrete structures built in aggressive and marine environments, affecting their structural performance and shortening their service lives. These challenges are discussed in detail in the next section as is addressing them.

Brittle failure behavior of steel-reinforced HCCs

HCCs have higher stiffness and flexural strength than SCCs with the same amount of concrete [5, 6]. Inadequate reinforcement details and low concrete strength [18] can, however, lead to the brittle failure of HCCs due to the reinforcement buckling or the concrete wall experiencing shear or crushing failure. The latter case is caused mostly by HCCs having thin concrete walls (high i/o ratio). A number of studies [4, 8] have suggested limiting the i/o ratio to 0.8 to ensure that HCCs have sufficient shear capacity. The brittle collapse of HCCs is due to buckling or yielding of the longitudinal bars when no additional resistance can be obtained due to the permanent deformation of the steel bars. In a well-detailed steel-reinforced HCC, the longitudinal bars are held together by the concrete wall and sufficiently confined by the lateral reinforcement until failure. Otherwise, insufficient lateral details result in premature elastic buckling of the longitudinal bars and a sudden loss in load-carrying capacity [71]. Because of this, plain-concrete HCCs encased within outer and inner steel or FRP tubes are currently being used to increase the strength performance of HCCs and to overcome the brittle behavior related

to the thin concrete wall [67]. These approaches, however, are difficult to implement and not cost-effective.

Steel-reinforcement corrosion in HCCs

The corrosion of steel reinforcement is becoming a crucial concern with HCCs due to their exposed inner and outer surfaces. Steel corrosion can dramatically reduce column strength and eliminate the confinement of the lateral reinforcement, leading to brittle failure [72, 73]. In fact, in efforts to extend their service lives, many steel-reinforced bridge piers are now being repaired or retrofitted because of significant steel corrosion problems [44, 49, 57, 71, 74, 75]. Maintaining these deteriorating structures is very expensive. Similar problems are now being experienced with hollow steel structures [76, 77]. Various techniques have been implemented to minimize deterioration of steel reinforcement such as the use of galvanizing, epoxy coating, and cathodic protection. Such alternatives are expensive and do not entirely eliminate steel corrosion [78]. There is a need therefore to explore the use of noncorroding reinforcement such as glass fiber-reinforced polymer (GFRP) bars in HCCs in order to mitigate the corrosion issues related to steel and to develop a more reliable and durable concrete structures.

CONCRETE COLUMNS REINFORCED WITH GFRP BARS

The use of glass fiber-reinforced polymer (GFRP) composite bars as internal reinforcement in concrete structures has increased in the last 30 years due to their many superior mechanical and environmental-resistance properties [16]. This type of reinforcement has been successfully implemented in concrete beams [17, 18], slabs [19, 20], and walls [21, 22]. The use of GFRP reinforcement for concrete columns has now become popular and effective [23-36]. The results of these studies demonstrated that, under axial loads, the concrete columns with GFRP longitudinal and transverse reinforcement had better and more stable behavior after the peak strength of the concrete or in the post-elastic stage than the steel-reinforced columns. Some studies [79-81] also recommend the use of GFRP reinforcement in concrete columns subject

to lateral and cyclic loads due to the high confinement efficiency provided by GFRP stirrups. Similar confinement efficiency and performance was found for GFRP-reinforced shear walls [22], demonstrating the high potential of using GFRP bars and stirrups for HCCs to overcome steel corrosion and obtain more reliable performance than steel-reinforced columns. Supporting these findings, a recent study [37] progressively investigated the behavior of the GFRP bars in compression where the test results showed significant axial resistance of these bars under compression. However, this axial resistance depends on the GFRP bar diameter and the length of the bar. Furthermore, this study provided a model to predict the maximum compressive strength of the GFRP bars accounting for different diameters and lengths, besides predicting their mode of failure.

Comparison between steel- and GFRP-reinforced SCCs: Overall behavior

Steel and GFRP bars have different material properties: the former has higher stiffness and elastic-plastic behavior before yielding, while the latter has higher strength and linear elastic behavior up to failure. **Figure 13** illustrates the typical load–strain behavior of a steel-reinforced SCC (**Figure 13a**) and a GFRP-reinforced SCC (**Figure 13b**). These examples are based on columns with the same dimensions (230 mm outer diameter), concrete compressive strength (32 MPa), and reinforcing details (6 12.7 mm longitudinal bars and 140 mm clear spacing between 10 mm lateral ligatures). The steel-reinforced column is modelled using the confinement model developed by Mander et al. [82], while the GFRP-reinforced column is modelled using the confinement model proposed by Karim et al. [36]. Both models express the compressive behavior of the confined SCCs with steel and GFRP reinforcement, respectively, and account for the lateral stress confinement provided by discrete lateral reinforcement. Both methods are based on the superposition of the constitutive material behavior such as the unconfined outer concrete cover, the inner confined concrete core, and the

reinforcing material: either steel bars ($E = 200$ GPa and $f_y = 400$ MPa) or GFRP bars ($E = 60$ GPa and $f_y = 1250$ MPa).

Based on **Figure 13**, the behavior of the unconfined outer concrete cover is similar for both columns and also from the columns modelled by Samani et al. [70], although the behavior of reinforcement and confined concrete differ. First, steel reinforcement has higher load contribution than GFRP bars due to its higher modulus of elasticity before yielding, denoted by the solid circle in **Figure 13a**. It should be noted that axial load contribution of the steel bars to the GFRP bars with the same cross-section is more than 3 ($= 200GPa/60GPa$) times at the peak load. Afterwards, the significant reduction in the stiffness of the longitudinal steel bars is caused by yielding, while the GFRP bars continuously withstand the axial loads with the same stiffness until failure. On the other hand, the confined concrete behavior in both columns shows a reduction after the peak strength due to the gradual spalling/crushing of the concrete core. The steel-reinforced SCCs have lower level of confinement due to the yielding of the lateral reinforcement, as denoted by the solid diamond shape in **Figure 13a**, compared to that of GFRP-reinforced SCCs. Overall, steel-reinforced SCC exhibits a higher strength capacity than the GFRP-reinforced SCC at the first peak (solid triangle). However, a stable load behavior after the first peak and further increase in the strength can be observed for GFRP-reinforced SCCs due to the linear elastic and high strength of GFRP bars.

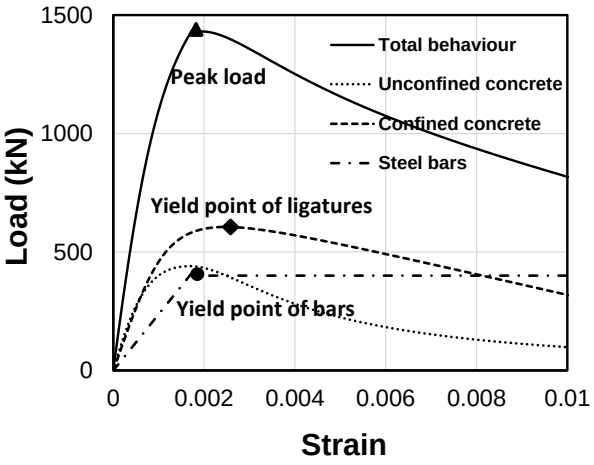

(a) Steel-reinforced SCCs

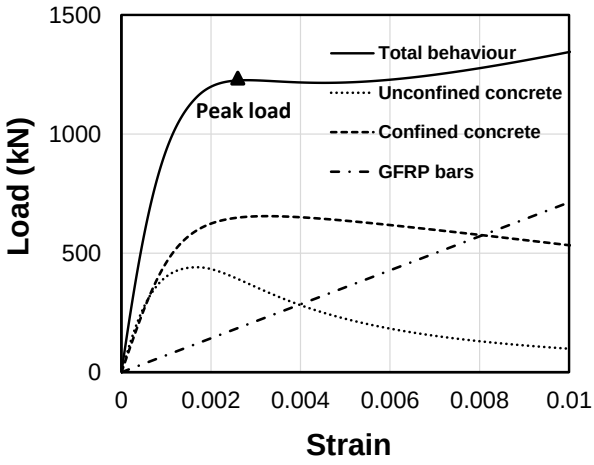

(b) GFRP-reinforced SCCs

Figure 13. Effect of reinforcing material on the behavior of SCCs

Comparison of experimental results: Axial-compressive loading behavior

A comprehensive evaluation of the concentric axial behavior of SCCs with steel and GFRP reinforcement published in the literature was conducted. It focused on the first peak strength (σ_1) (the first peak strength after the elastic state), the confined strength (σ_2) (the strength induced by the concrete core due to lateral confinement), and the axial-displacement capacity. A total of 10 experimental studies were reviewed representing 20 columns and their results are summarized in **Table 6**. **Figure 14** shows the comparison between the investigated parameters for both reinforcing systems. In **Figure 14a**, all of the studies showed that the σ_1 of the steel-reinforced SCCs was higher than that of the GFRP-reinforced SCCs. This is due to the higher modulus of the longitudinal steel bars, contributing almost 10% to 28%, while the lower modulus of the GFRP bars contributed only 3% to 14% (**Table 6**). In contrast, **Figure 14b** shows that the GFRP-reinforced SCCs had higher confined strength (σ_2/f_c') than the steel-reinforced columns. This finding can be explained by the higher strength and linear elastic behavior of the GFRP bars up to failure, unlike steel reinforcement, which cannot resist additional load after yielding. The load contribution of the GFRP bars at failure was therefore 50% higher than that of the steel bars [29]. Moreover, the lateral GFRP reinforcement provided higher confining stress than the steel bars. The confinement provided by the linear elastic GFRP ligatures increased with the load, while the confinement provided by the steel ligatures was the same after yielding. On the other hand, the experimental results in **Figure 14c** show that the GFRP-reinforced SCCs exhibited more deformation before failing than their steel-reinforced counterparts. This can also be attributed to the linear elastic behavior of GFRP reinforcement: the crushing strain of GFRP bars is four to five times higher than the yield strain of steel bars [27].

Table 6. Experimental studies compared the axial behavior between steel and GFRP-reinforced SCCs

Authors	f_c'	Load Contribution at σ_1 (%)		Maximum Axial-Load Ratio (σ_1/f_c')		Confinement Efficiency (σ_2/f_c')		Displacement Capacity	
	(MPa)	Steel	GFRP	Steel	GFRP	Steel	GFRP	Steel	GFRP
De Luca et al. [32]	34.5	11.6	4.2	0.90	0.88	-	-	1.36	1.97
Tobbi et al. [24]	32.6	12.0	10.0	1.05	0.99	1.26	1.36	-	-
Afifi et al. [23]	42.9	15.0	9.0	1.05	0.98	1.69	1.74	1.90	2.00
Pantelides et al. [73]	36.0	11.1	3.2	1.22	1.08	1.35	1.36	2.70	3.60
Mohammad et al. [83]	42.9	15.0	8.0	1.04	0.96	1.69	1.74	1.90	2.00
Hadi et al. [29]	37.0	26.6	13.4	1.25	1.00	1.37	1.50	8.70	9.00
Hales et al. [84]	90.0	-	-	1.09	1.02	-	-	-	-
Elchalakani and Ma [85]	32.8	15.8	3.2	1.13	1.06	2.60	2.46	1.10	1.50
Hasan et al. [86]	85.0	10.1	6.7	0.93	0.92	1.13	1.13	3.30	2.60
Al-Shareedah [87]	30.0	27.8	11.8	0.96	0.96	1.27	1.55	2.00	2.27

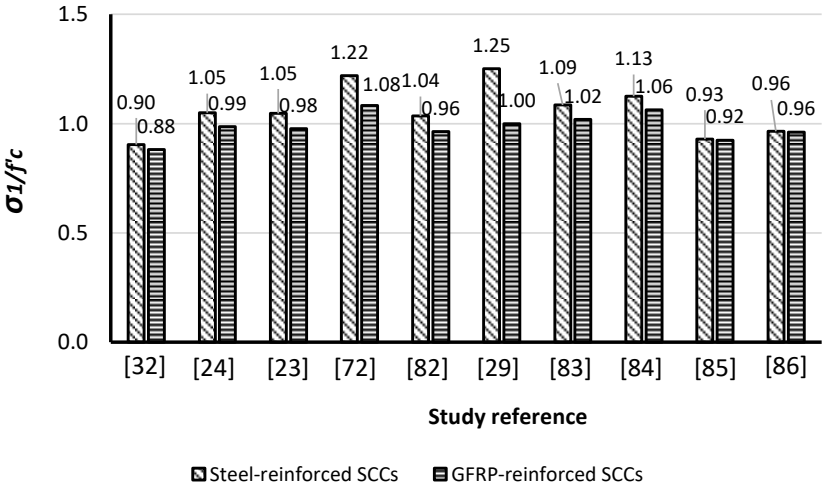

(a) (σ_1/f_c')

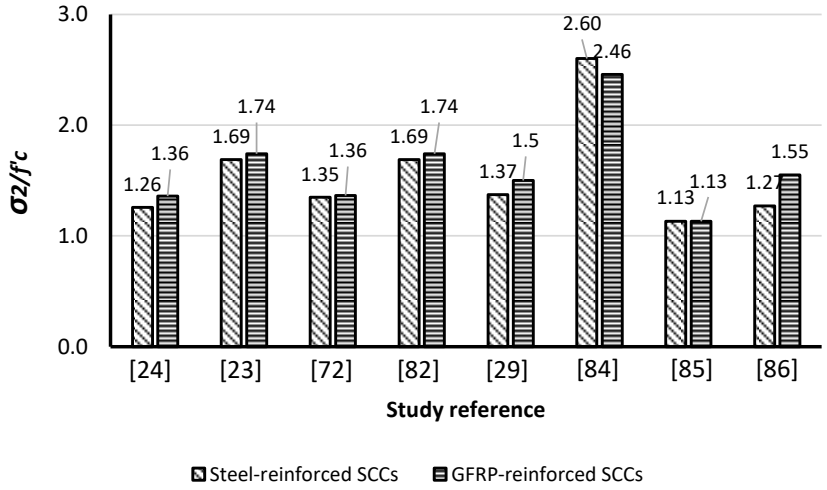

(b) (σ_2/f_c')

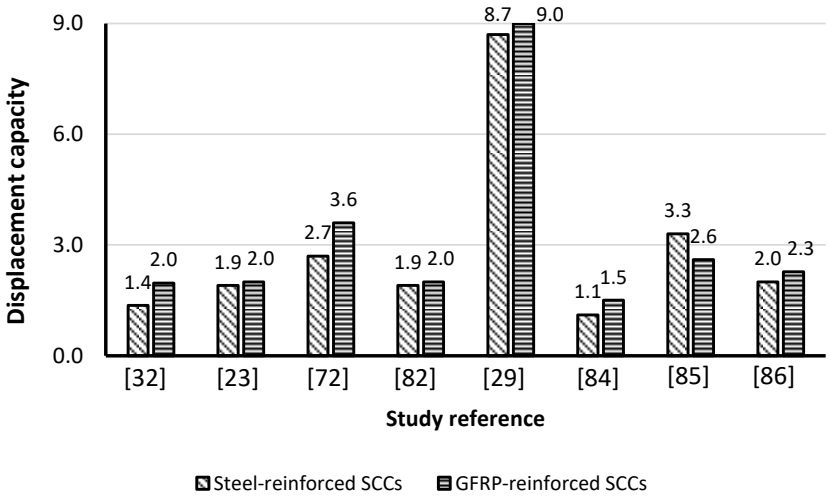

(c) Displacement capacity

Figure 14. Effect of reinforcing material on the axial behavior of SCCs

Comparison of experimental results: Hysteretic loading behavior

HCC behavior has been investigated primarily under hysteretic loading, as shown in **Figure 4a**. **Table 7** summarizes the test results in the literature on GFRP reinforcement in SCCs and concrete walls, as well as comparisons with their steel-reinforced counterparts. For the columns tested under axial lateral loads, the most investigated behaviors were ductility (μ_Δ) and lateral-load capacity. For direct comparison, the bending moment (M) was calculated by multiplying the lateral load by the column height. The confined strength ($\sigma_c = Mc/I_{cr}$) was then derived and normalized based on the concrete compressive strength (f_c'). In the calculation of σ_c, c is the mid-height of the section (mm) in the direction of loading and I_{cr} is the moment of inertia of the cracked section approximated as $0.35I_g$ (I_g is the gross moment of inertia of the section) [88]. It should be mentioned that c assumed to be the mid-height of the section even with the cracked section just to ease comparing between the columns with the two reinforcing systems where this value applied equally for both and it is hard to be exactly calculated. The test results in **Figure 15a** show that using GFRP reinforcement enhanced the lateral-load capacity and confined strength by up to 22%. The columns with steel bars, however, evidenced more energy

dissipation [89, 90]. The behavioral difference between these reinforcing materials is the main reason behind these findings: the steel-reinforced columns exhibited strength degradation after the yielding of the steel and failed due to buckling of longitudinal steel bars. On the other hand, the GFRP-reinforced columns experienced no strength degradation due to their linear elastic behavior up to failure. Concrete crushing at advanced loading levels, however, caused splitting in the longitudinal GFRP bars. **Figure 15b** shows higher ductility in the GFRP-reinforced SCCs and concrete walls compared to the steel-reinforced ones. This behavior can be attributed to the GFRP bars having higher strain at failure than the steel bars. Moreover, the ductility is controlled primarily by the reinforcement ratio and the spacing between the lateral reinforcement: a decrease in reinforcement or increase in spacing can cause splitting failure in longitudinal GFRP bars [81, 91].

Table 7. Experimental studies comparing the hysteretic behavior between steel- and GFRP-reinforced SCCs

Authors	Sample Name		μ_Δ		σ_c/f'_c	
	Steel	**GFRP**	**Steel**	**GFRP**	**Steel**	**GFRP**
Nayera et al. [22]	ST15	G15	2.6	3.1	1.59	1.96
Tavassoli et al. [89, 90]	P28-LS-12-50-7	P28-B-12-50	4.7	9.2	2.06	2.16
	P40-LS-12-160-6	P42-C12-160	3.1	3.7	0.93	1.05
Ali and El-salakawy [81]	S-1.3-10-75	G-1.3-10-75	8.5	12.5	1.54	1.83
Elshamandy et al. [91]	ST12N10-C4-100	G12N13-C4-100	7.7	10.4	2.35	2.36
	ST8N10-C1-100	G8N13-C1-100	6.6	5.5	1.98	2.22
Arafa et al. [92]	SX4	GX4	2.0	3.0	1.16	1.74
Deng et al. [93]	6SG-120	2GG-120	4.78	1.57	1.88	1.77
	11SG-120	9GG-120	4.68	1.58	1.31	1.36

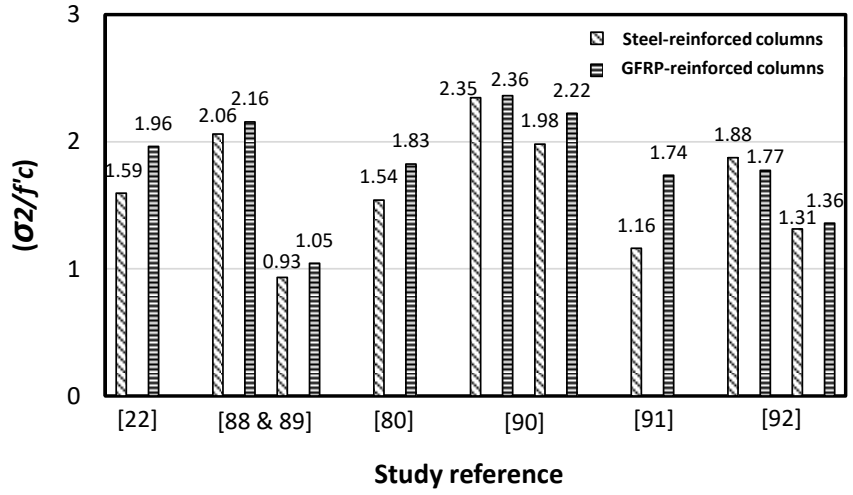

(a) (σ_c/f_c')

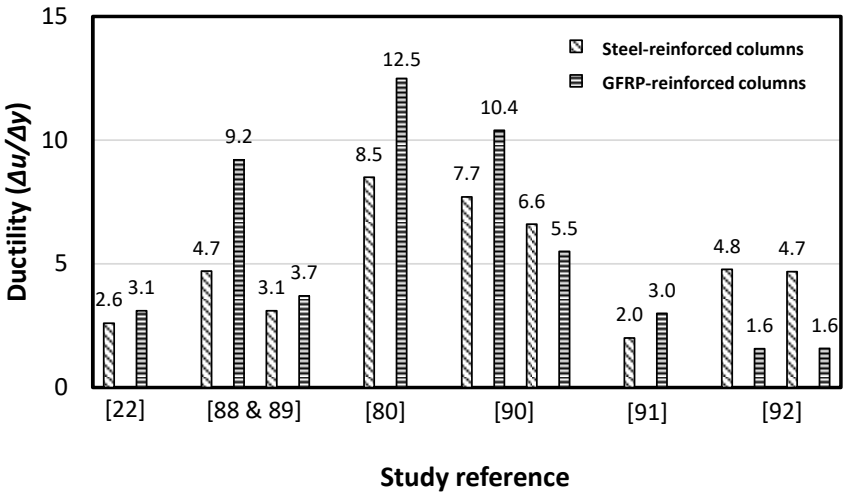

(b) Ductility

Figure 15. Effect of reinforcing material on the hysteretic behavior of SCCs

Benefits of using GFRP bars in SCCs

The reviewed experimental studies showed the benefits and effectiveness of using GFRP bars as internal reinforcement in SCCs subject to axial and cyclic loading. Furthermore, GFRP bars were found to be suitable for SCCs in mitigating strength degradation after concrete cover spalling due to their high strength and linear elastic behavior up failure. Moreover, the linear elastic nature of GFRP reinforcement, combined with the nonlinear behavior of concrete in compression and their relatively close moduli of elasticity, can provide a reinforced-concrete column with better overall performance and higher deformation capacity with a more

progressive failure behavior than steel-reinforced SCCs. These positive attributes would be beneficial in addressing the limited performance of steel-reinforced HCCs. Therefore, the potential of GFRP bars and spirals as reinforcing materials for hollow concrete columns should be explored and their axial behavior should be investigated as a first step in understanding the structural performance of this construction system.

GFRP BARS AS REINFORCEMENT FOR HCCs

Results of recent investigations

Most research and developments on concrete structures reinforced with GFRP bars have focused solely on SCCs. The authors, however, recently undertook pioneering experimental and analytical work on GFRP-reinforced HCCs. Experimental investigations on the concentric compressive behavior of GFRP-reinforced HCCs considering different design parameters such as the inner-to-outer diameter ratio (i/o) ratio [34], reinforcement ratio (ρ) [33], volumetric ratio (ρ_v), and concrete compressive strength (f_c') (the work is under review) were implemented. These studies found that increasing the i/o ratio in GFRP-reinforced HCCs resulted in more stable load–deformation behavior than in GFRP-reinforced SCCs and steel-reinforced HCCs by increasing the displacement capacity and confined strength (see **Figure 16a**). This behavior contradicts that reported by Fam and Rizkalla [38] and Micelli and Modarelli [45], namely that increasing the (i/o) ratio decreased the strength in plain-concrete HCCs due to increase the shear effect on the thinner unreinforced concrete wall. GFRP bars as internal reinforcement in HCCs improves their performance due to GFRP's elastic linear behavior. This provides for maintaining the strength in concrete columns with higher (i/o) ratios and overcomes the brittle failure caused by crushing of the inner concrete wall. In the same study, Alajarmeh et al. [34] evaluated the effect of using longitudinal steel and GFRP bars in HCCs. The results show that the steel-reinforced HCCs behaved the same behavior as the columns tested by Kusumawardaningsih and Hadi [2], and Yazici [50], who observed a

reduction in compressive strength after the peak. In contrast, the GFRP-reinforced HCCs exhibited a strength increase after the first peak without any degradation and significantly high deformation before failure.

The increase in ρ achieved by increasing the number of longitudinal bars led to a significant increase in the confined strength but had no effect on the displacement capacity, as the longitudinal GFRP bars had a crushing strain almost same as that of the concrete [33] (see **Figure 16b**). These findings are consistent with the observations of Afifi et al. [23] and Tobbi et al. [26] for GFRP-reinforced SCCs. On the other hand, closely spaced lateral reinforcement delayed failure and increased both displacement capacity and confined strength (**Figure 16c**). This is due to the GFRP lateral reinforcement increasing the concrete confinement. GFRP spirals with a small spacing also provided higher strength and displacement than the steel-reinforced HCCs wrapped with CFRP sheets—based on Kusumawardaningsih and Hadi [2] and Yazici [50]—and higher than the GFRP-reinforced SCCs with close lateral reinforcement—based on Afifi et al. [23] and Maranan et al. [27]. In contrast, the GFRP-reinforced HCCs experienced reduced displacement capacity and an insignificant decrease in confined strength (see **Figure 16d**), when the concrete compressive strength (f_c') was high. This is due to the increased brittleness of high compressive strength concrete. This finding is consistent with [45], as shown in **Figure 10b**, where the increase in f_c' decreased the displacement capacity of the HCCs. Moreover, using GFRP bars and concrete with high f_c' in HCCs (**Figure 16d**) can maintain the confined strength, whereas a reduction was observed in the HCCs with higher concrete strength (see **Figure 10b**).

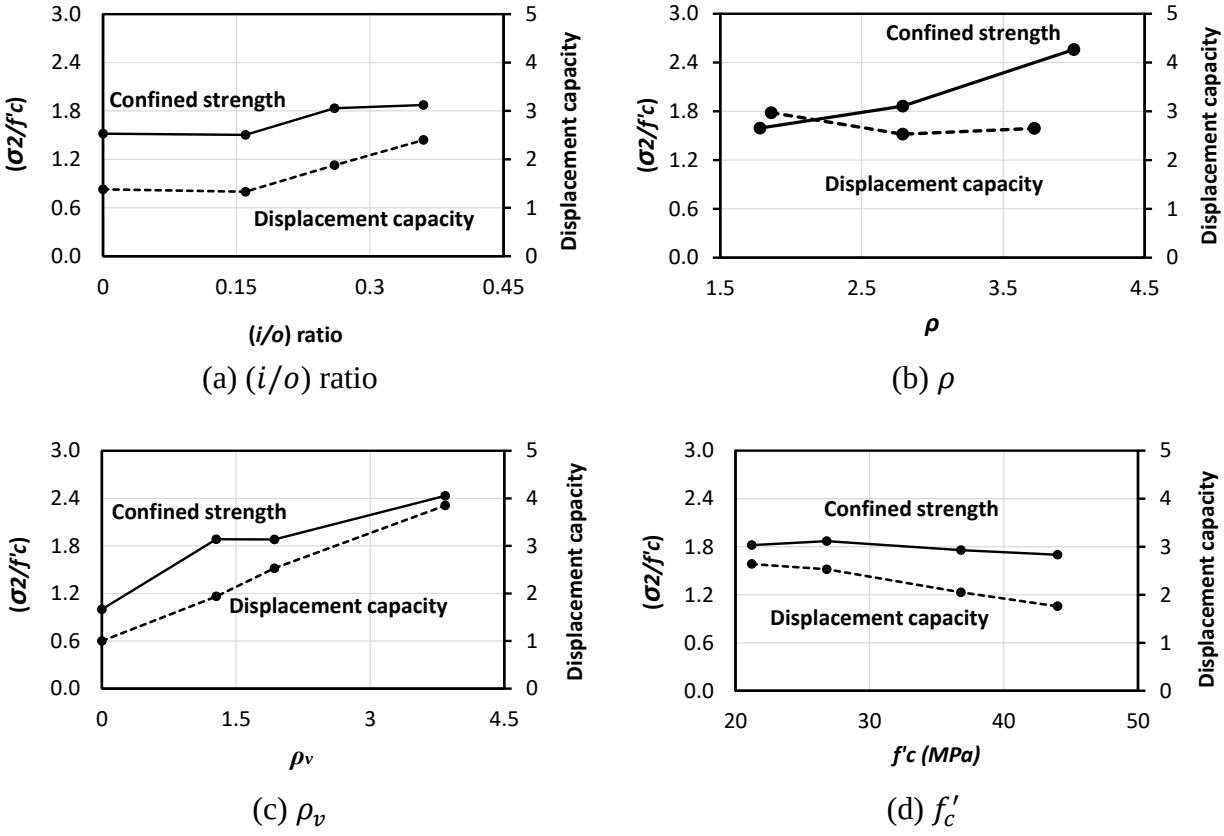

(a) (i/o) ratio (b) ρ

(c) ρ_v (d) f_c'

Figure 16. Effect of the design parameters on the behavior of GFRP-reinforced HCCs

New opportunities and future research on GFRP-reinforced HCCs

The effects of different design parameters have been well investigated and studied for HCCs with steel reinforcement. Some techniques have also been suggested to improve the performance and enhance the ductility of HCCs, including the use of multilayers of longitudinal reinforcement, changing the lateral-reinforcement configuration, and wrapping the outer face of the HCCs with FRP sheets. While such techniques have significantly improved the behavior of HCCs, the corrosion of steel bars remains a significant issue in steel-reinforced HCCs.

The effectiveness of GFRP reinforcement in SCCs, as shown by the results on the recent work on the GFRP-reinforced HCCs (**Figure 16**), demonstrates the high potential for extensively

investigating the behavior of this new construction system to develop noncorroding, structurally reliable civil-engineering structures.

The use of GFRP bars is anticipated to increase the ductility and strength of HCCs to take advantage of their high strength and strain capacities. These qualities allow GFRP reinforcement to contribute continuously in carrying the applied load with concrete until failure, resulting in a better stress distribution inside HCCs and leading to significantly enhanced overall performance. Moreover, this system may provide a better solution than wrapping the outer surface of steel-reinforced HCCs with FRP or using the double-skin tube system, because it will totally eliminate the corrosion issue and be a more effective construction method.

CONCLUSIONS

This state-of-the-art review on hollow concrete columns identified the critical design parameters and their structural performance under different loading conditions. The challenges and opportunities in using GFRP reinforcement in this type of construction system were also critically analyzed. Based on this extensive review and analysis, the following conclusions can be drawn:

1. The use of hollow concrete columns is drawing growing interest, as shown by the greater number of relevant studies in the last 10 years. From 1993 to 2018, there were 41 reported studies on HCCs investigating the behavior of this construction system under different loading conditions and with different design parameters.
2. The behavior of HCCs has been widely investigated under hysteretic and axial loading conditions, representing 87% of the total number of studies, as these loading conditions are required in designing bridge piers. Moreover, the ratio of the inner-to-outer diameter, reinforcement ratio, volumetric ratio, and concrete compressive strength have

been identified as the most critical and well-investigated design parameters primarily affecting the structural performance of steel-reinforced hollow concrete columns.

3. The overall behavior of steel-reinforced HCCs is significantly different than that of SCCs due to the absence of the concrete core, which changes the inner stress formation from triaxial in the latter to biaxial in the former. This change reduces the lateral expansion of the cross section in the former, leading to more axial stability to achieve greater axial deformation. Therefore, the capacity of HCCs is comparable to or even higher than their solid counterparts when the appropriate levels of design parameters are used.
4. Steel-reinforced hollow concrete columns typically failed in a brittle manner due to either crushing of inner concrete core or buckling/yielding of the longitudinal bars. Steel-reinforced HCCs can be effectively designed by providing adequate inner-wall thickness (less than 0.8) or sufficient spacing between lateral reinforcement.
5. Glass fiber-reinforced (GFRP) bars can be the solution to overcome the brittle behavior of steel-reinforced HCCs. The linear elastic nature of GFRP bars, combined with the nonlinear behavior of concrete in compression and their relatively close moduli of elasticity, can provide HCCs with a higher deformation capacity and a more progressive failure behavior than steel-reinforced HCCs. In addition to using GFRP bars, creating a hollow section inside the concrete column leads to higher deformation capacity than in SCCs due to the lower lateral expansion and, therefore, GFRP-reinforced HCCs would be a good solution to overcome the brittle behavior of such columns.
6. Preliminary investigations indicate that GFRP-reinforced hollow concrete columns will benefit from the high strength and strain capacities of GFRP bars. This new construction system has exhibited higher strength and ductility than steel-reinforced

columns due to the better stress distribution within the hollow concrete wall, leading to a significant enhancement in overall performance.

The outcomes of this review also point to opportunities and new research areas that can be explored to further understand how the critical design parameters affect the structural performance of GFRP-reinforced hollow concrete columns. Moreover, the behavior of GFRP-reinforced hollow concrete columns under the different loading conditions in which this construction system is heavily used should be investigated. The results of these investigations will be useful in revealing the many benefits of this new construction system and to provide useful information to support the work of the technical committees engaged in the development of standards and design provisions for GFRP-reinforced concrete columns.

ACKNOWLEDGEMENTS

The first author gratefully acknowledges Tafila Technical University, the University of Southern Queensland, and the Natural Science and Research Council of Canada (NSERC) for their financial support. The assistance from the Centre of Future Materials (CFM) is also acknowledged.

REFERENCES

1. Lignola, G.P., et al., *Experimental performance of RC hollow columns confined with CFRP.* Journal of Composites for Construction, 2007. **11**(1): p. 42-49.
2. Kusumawardaningsih, Y. and M.N. Hadi, *Comparative behaviour of hollow columns confined with FRP composites.* Composite Structures, 2010. **93**(1): p. 198-205.
3. Mander, J.B., *Seismic design of bridge piers.* 1983.
4. Zahn, F., *Design of reinforced concrete bridge columns for strength and ductility.* 1986.
5. Whittaker, D., *Seismic performance of offshore concrete gravity platforms.* 1987.
6. Lee, J.-H., et al., *Seismic performance of circular hollow RC bridge columns.* KSCE Journal of Civil Engineering, 2015. **19**(5): p. 1456-1467.
7. Hoshikuma, J. and M. Priestley, *Flexural behavior of circular hollow columns with a single layer of reinforcement under seismic loading.* SSRP, 2000: p. 13.
8. Ranzo, G. and M.N. Priestley, *Seismic performance of circular hollow columns subjected to high shear*. 2001: Structural Systems Research Project, University of California, San Diego.

9. Yeh, Y.-K., Y. Mo, and C. Yang, *Seismic performance of hollow circular bridge piers.* Structural Journal, 2001. **98**(6): p. 862-871.
10. Yeh, Y.-K., Y.L. Mo, and C. Yang, *Seismic performance of rectangular hollow bridge columns.* Journal of Structural Engineering, 2002. **128**(1): p. 60-68.
11. Osada, K., T. Yamaguchi, and S. Ikeda, *Seismic performance and the strengthening of hollow circular RC piers having reinforced cut-off planes and variable wall thickness.* Concrete Res. and Tech, 1999. **101**: p. 13-24.
12. Mo, Y., D. Wong, and K. Maekawa, *Seismic performance of hollow bridge columns.* Structural Journal, 2003. **100**(3): p. 337-348.
13. Pinto, A., J. Molina, and G. Tsionis, *Cyclic tests on large-scale models of existing bridge piers with rectangular hollow cross-section.* Earthquake engineering & structural dynamics, 2003. **32**(13): p. 1995-2012.
14. Pavese, A., D. Bolognini, and S. Peloso, *FRP seismic retrofit of RC square hollow section bridge piers.* Journal of earthquake engineering, 2004. **8**(spec01): p. 225-250.
15. Liang, X., R. Beck, and S. Sritharan, *Understanding the Confined Concrete Behavior on the Response of Hollow Bridge Columns*, in *Department of Civil, Construction and Environmental Engineering*. 2015, Iowa State University: California Department of Transportation.
16. Manalo, A., et al., *Recent developments on FRP bars as internal reinforcement in concrete structures.* Concrete in Australia, 2014. **40**(2): p. 46-56.
17. El-Nemr, A., E.A. Ahmed, and B. Benmokrane, *Flexural Behavior and Serviceability of Normal-and High-Strength Concrete Beams Reinforced with Glass Fiber-Reinforced Polymer Bars.* ACI structural journal, 2013. **110**(6).
18. Maranan, G., et al., *Evaluation of the flexural strength and serviceability of geopolymer concrete beams reinforced with glass-fibre-reinforced polymer (GFRP) bars.* Engineering Structures, 2015. **101**: p. 529-541.
19. Michaluk, C.R., et al., *Flexural behavior of one-way concrete slabs reinforced by fiber reinforced plastic reinforcements.* ACI Structural Journal, 1998. **95**: p. 353-365.
20. El-Sayed, A., E. El-Salakawy, and B. Benmokrane, *Shear strength of one-way concrete slabs reinforced with fiber-reinforced polymer composite bars.* Journal of Composites for Construction, 2005. **9**(2): p. 147-157.
21. Hassanein, A., et al., *STR-830: Enhancing the deformation capacity of concrete shear walls reinforced with GFRP bars.* 2016.
22. Mohamed, N., et al., *Experimental investigation of concrete shear walls reinforced with glass fiber–reinforced bars under lateral cyclic loading.* Journal of Composites for Construction, 2014. **18**(3): p. A4014001.
23. Afifi, M.Z., H.M. Mohamed, and B. Benmokrane, *Axial capacity of circular concrete columns reinforced with GFRP bars and spirals.* Journal of Composites for Construction, 2013. **18**(1).
24. Tobbi, H., A.S. Farghaly, and B. Benmokrane, *Concrete columns reinforced longitudinally and transversally with glass fiber-reinforced polymer bars.* ACI Structural Journal, 2012. **109**(4): p. 551.
25. Alsayed, S., et al., *Concrete columns reinforced by glass fiber reinforced polymer rods.* Special Publication, 1999. **188**: p. 103-112.
26. Tobbi, H., A.S. Farghaly, and B. Benmokrane, *Behavior of concentrically loaded fiber-reinforced polymer reinforced concrete columns with varying reinforcement types and ratios.* ACI Structural Journal, 2014. **111**(2): p. 375.
27. Maranan, G., et al., *Behavior of concentrically loaded geopolymer-concrete circular columns reinforced longitudinally and transversely with GFRP bars.* Engineering Structures, 2016. **117**: p. 422-436.

28. Zadeh, H.J. and A. Nanni, *Design of RC columns using glass FRP reinforcement.* Journal of Composites for Construction, 2012. **17**(3): p. 294-304.
29. Hadi, M.N., H. Karim, and M.N. Sheikh, *Experimental investigations on circular concrete columns reinforced with GFRP bars and helices under different loading conditions.* Journal of Composites for Construction, 2016. **20**(4).
30. Hadi, M.N., H.A. Hasan, and M.N. Sheikh, *Experimental Investigation of Circular High-Strength Concrete Columns Reinforced with Glass Fiber-Reinforced Polymer Bars and Helices under Different Loading Conditions.* Journal of Composites for Construction, 2017: p. 04017005.
31. Hadhood, A., H.M. Mohamed, and B. Benmokrane, *Experimental Study of Circular High-Strength Concrete Columns Reinforced with GFRP Bars and Spirals under Concentric and Eccentric Loading.* Journal of Composites for Construction, 2016: p. 04016078.
32. De Luca, A., F. Matta, and A. Nanni, *Behavior of full-scale glass fiber-reinforced polymer reinforced concrete columns under axial load.* ACI Structural Journal, 2010. **107**(5): p. 589.
33. AlAjarmeh, O.S., et al., *Axial performance of hollow concrete columns reinforced with GFRP composite bars with different reinforcement ratios.* Composite Structures, 2019b. **213**(1): p. 12.
34. AlAjarmeh, O.S., et al., *Compressive behavior of axially loaded circular hollow concrete columns reinforced with GFRP bars and spirals.* Construction and Building Materials, 2019a. **194**: p. 12-23.
35. Hadhood, A., et al., *Efficiency of glass-fiber reinforced-polymer (GFRP) discrete hoops and bars in concrete columns under combined axial and flexural loads.* Composites Part B: Engineering, 2017. **114**: p. 223-236.
36. Karim, H., M.N. Sheikh, and M.N. Hadi, *Axial load-axial deformation behaviour of circular concrete columns reinforced with GFRP bars and helices.* Construction and Building Materials, 2016. **112**: p. 1147-1157.
37. O.S. AlAjarmeh, A.C.M., B. Benmokrane, P.V. Vijay, W. Ferdous, P. Mendis, *Novel testing and characterization of GFRP bars in compression.* Construction and Building Materials, 2019. **Volume 225**: p. Pages 1112-1126.
38. Fam, A. and S.H. Rizkalla, *Behavior of axially loaded concrete-filled circular FRP tubes.* ACI Structural Journal, 2001. **98**(3): p. 280-289.
39. Liang, X. and S. Sritharan, *Effects of Confinement in Circular Hollow Concrete Columns.* Journal of Structural Engineering, 2018. **144**(9): p. 04018159.
40. Zahn, F., R. Park, and M. Priestley, *Flexural strength and ductility of circular hollow reinforced concrete columns without confinement on inside face.* Structural Journal, 1990. **87**(2): p. 156-166.
41. Kishida, S., et al., *Experimental study on shear strength of the PHC pile with large diameter.* J Struct. Const. Eng, 1998. **8**(519): p. 123-130.
42. Mo, Y. and I. Nien, *Seismic performance of hollow high-strength concrete bridge columns.* Journal of Bridge Engineering, 2002. **7**(6): p. 338-349.
43. Calvi, G.M., et al., *Experimental and numerical studies on the seismic response of RC hollow bridge piers.* Bulletin of Earthquake Engineering, 2005. **3**(3): p. 267-297.
44. Modarelli, R., F. Micelli, and O. Manni. *FRP-confinement of hollow concrete cylinders and prisms*. in *Proceedings of the 7th International Symposium on FRP reinforcement for reinforced concrete structures, Kansas City, Missouri*. 2005. Citeseer.

45. Micelli, F. and R. Modarelli, *Experimental and analytical study on properties affecting the behaviour of FRP-confined concrete.* Composites Part B: Engineering, 2013. **45**(1): p. 1420-1431.
46. Yeh, Y.-K. and Y. Mo, *Shear retrofit of hollow bridge piers with carbon fiber-reinforced polymer sheets.* Journal of Composites for Construction, 2005. **9**(4): p. 327-336.
47. Delgado, P., *Avaliação da Segurança Estrutural em Pontes*. 2008, PhD Thesis, FEUP, Porto (in Portuguese).
48. Turmo, J., G. Ramos, and A. Aparicio, *Shear truss analogy for concrete members of solid and hollow circular cross section.* Engineering Structures, 2009. **31**(2): p. 455-465.
49. Lignola, G.P., et al., *Analysis of RC Hollow Columns Strengthened with GFRP.* Journal of Composites for Construction, 2011. **15**(4): p. 545-556.
50. Yazici, V., *Strengthening hollow reinforced concrete columns with fibre reinforced polymers*. 2012, University of Wollongong.
51. Kim, I.-H., C.-H. Sun, and M. Shin, *Concrete contribution to initial shear strength of RC hollow bridge columns.* 2012.
52. Cheon, J.-H., et al., *Inelastic behaviour and ductility capacity of circular hollow reinforced concrete bridge piers under earthquake.* Magazine of concrete Research, 2012. **64**(10): p. 919-930.
53. Kim, T.-H., et al., *Performance assessment of hollow RC bridge column sections with reinforcement details for material quantity reduction.* Magazine of Concrete Research, 2013. **65**(21): p. 1277-1292.
54. Han, Q., et al., *Experimental study of hollow rectangular bridge column performance under vertical and cyclically bilateral loads.* Earthquake Engineering and Engineering Vibration, 2013. **12**(3): p. 433-445.
55. Zhang, Y.-y., K.A. Harries, and W.-c. Yuan, *Experimental and numerical investigation of the seismic performance of hollow rectangular bridge piers constructed with and without steel fiber reinforced concrete.* Engineering Structures, 2013. **48**: p. 255-265.
56. Shin, M., et al., *Effectiveness of low-cost fiber-reinforced cement composites in hollow columns under cyclic loading.* Construction and Building Materials, 2013. **47**: p. 623-635.
57. Hadi, M. and T. Le, *Behaviour of hollow core square reinforced concrete columns wrapped with CFRP with different fibre orientations.* Construction and Building Materials, 2014. **50**: p. 62-73.
58. Han, Q., et al., *Experimental and numerical studies on seismic behavior of hollow bridge columns retrofitted with carbon fiber reinforced polymer.* Journal of Reinforced Plastics and Composites, 2014. **33**(24): p. 2214-2227.
59. Völgyi, I., A. Windisch, and G. Farkas, *Resistance of reinforced concrete members with hollow circular cross-sections under combined bending and shear–Part I: experimental investigation.* Structural Concrete, 2014. **15**(1): p. 13-20.
60. Kim, T.-H., J.-H. Lee, and H.M. Shin, *Performance assessment of hollow RC bridge columns with triangular reinforcement details.* Magazine of Concrete Research, 2014. **66**(16): p. 809-824.
61. Prado, N.I., et al., *Arrangement of Transverse Reinforcement in Hollow Piers Subjected to Lateral Load.* ACI Structural Journal, 2016. **113**(4): p. 723.
62. Cassese, P., P. Ricci, and G.M. Verderame, *Experimental study on the seismic performance of existing reinforced concrete bridge piers with hollow rectangular section.* Engineering Structures, 2017. **144**: p. 88-106.

63. Jameel, M.T., M.N. Sheikh, and M.N. Hadi, *Behaviour of circularized and FRP wrapped hollow concrete specimens under axial compressive load.* Composite Structures, 2017. **171**: p. 538-548.
64. Hadi, M.N., M.T. Jameel, and M.N. Sheikh, *Behavior of circularized hollow RC columns under different loading conditions.* Journal of Composites for Construction, 2017. **21**(5): p. 04017025.
65. Cassese, P., M.T. De Risi, and G.M. Verderame, *Seismic assessment of existing hollow circular reinforced concrete bridge piers.* Journal of Earthquake Engineering, 2018: p. 1-36.
66. Irawan, C., et al., *Confinement Behavior of Spun Pile using Low Amount of Spiral Reinforcement–an Experimental Study.* International Journal on Advanced Science, Engineering and Information Technology, 2018. **8**(2): p. 501-507.
67. Al-saadi, A.U., T. Aravinthan, and W. Lokuge, *Structural applications of fibre reinforced polymer (FRP) composite tubes: A review of columns members.* Composite Structures, 2018.
68. Han, T., et al., *Nonlinear concrete model for an internally confined hollow reinforced concrete column.* Magazine of Concrete Research, 2008. **60**(6): p. 429-440.
69. Simmons, J., *Poisson's ratio of concrete: a comparison of dynamic and static measurements.* Magazine of Concrete Research, 1955. **7**(20): p. 61-68.
70. Samani, A.K. and M.M. Attard, *A stress–strain model for uniaxial and confined concrete under compression.* Engineering Structures, 2012. **41**: p. 335-349.
71. Lignola, G., et al., *Analysis of the confinement of RC hollow columns wrapped with FRP.* Materials Characterization, 2007. **3**(S3): p. 300.
72. Li, J., J. Gong, and L. Wang, *Seismic behavior of corrosion-damaged reinforced concrete columns strengthened using combined carbon fiber-reinforced polymer and steel jacket.* Construction and Building Materials, 2009. **23**(7): p. 2653-2663.
73. Pantelides, C.P., M.E. Gibbons, and L.D. Reaveley, *Axial load behavior of concrete columns confined with GFRP spirals.* Journal of Composites for Construction, 2013. **17**(3): p. 305-313.
74. Yazici, V. and M.N. Hadi, *Axial load-bending moment diagrams of carbon FRP wrapped hollow core reinforced concrete columns.* Journal of Composites for Construction, 2009. **13**(4): p. 262-268.
75. Falsafi, T., et al., *Experimental Study on Behaviour of Prismatic and Cylindrical Hollow Concrete Columns Reinforced with FRP Materials.* 2010.
76. Zhao, X.-L. and L. Zhang, *State-of-the-art review on FRP strengthened steel structures.* Engineering Structures, 2007. **29**(8): p. 1808-1823.
77. Elchalakani, M., *Rehabilitation of corroded steel CHS under combined bending and bearing using CFRP.* Journal of Constructional Steel Research, 2016. **125**: p. 26-42.
78. Nkurunziza, G., et al., *Durability of GFRP bars: a critical review of the literature.* Progress in structural engineering and materials, 2005. **7**(4): p. 194-209.
79. Tavassoli, A., *Behaviour of Circular Concrete Columns Internally Reinforced with Steel and GFRP under Combined Axial Load and Bending*, in *Master of Applied Science in Civil Engineering*. 2015, University of Toronto.
80. Tavassoli, A. and S.A. Sheikh, *Seismic Resistance of Circular Columns Reinforced with Steel and GFRP.* Journal of Composites for Construction, 2017. **21**(4): p. 04017002.
81. Ali, M.A. and E. El-Salakawy, *Seismic performance of GFRP-reinforced concrete rectangular columns.* Journal of Composites for Construction, 2015. **20**(3): p. 04015074.

82. Mander, J.B., M.J. Priestley, and R. Park, *Theoretical stress-strain model for confined concrete.* Journal of structural engineering, 1988. **114**(8): p. 1804-1826.
83. Mohamed, H.M., M.Z. Afifi, and B. Benmokrane, *Performance evaluation of concrete columns reinforced longitudinally with FRP bars and confined with FRP hoops and spirals under axial load.* Journal of Bridge Engineering, 2014. **19**(7): p. 04014020.
84. Hales, T.A., C.P. Pantelides, and L.D. Reaveley, *Experimental evaluation of slender high-strength concrete columns with GFRP and hybrid reinforcement.* Journal of Composites for Construction, 2016. **20**(6): p. 04016050.
85. Elchalakani, M. and G. Ma, *Tests of glass fibre reinforced polymer rectangular concrete columns subjected to concentric and eccentric axial loading.* Engineering Structures, 2017. **151**: p. 93-104.
86. Hasan, H.A., M.N. Sheikh, and M.N. Hadi, *Performance evaluation of high strength concrete and steel fibre high strength concrete columns reinforced with GFRP bars and helices.* Construction and Building Materials, 2017. **134**: p. 297-310.
87. Othman S. Al-Shareedah, *Performance Evaluation of Axially Loaded Circular GFRP-Reinforced Concrete Columns*, in *Civil and Architectural Engineering Department*. 2016, Sultan Qaboos University: Oman.
88. ACI, *(American Concrete Institute), Building code requirements for structural concrete.* ACI 318-14M, Farmington Hills, MI, 2014.
89. Tavassoli, A. and S.A. Sheikh, *Seismic Resistance of Circular Columns Reinforced with Steel and GFRP.* Journal of Composites for Construction, 2017: p. 04017002.
90. Tavassoli, A., J. Liu, and S. Sheikh, *Glass fiber-reinforced polymer-reinforced circular columns under simulated seismic loads.* ACI Structural Journal, 2015. **112**(1): p. 103.
91. Elshamandy, M.G., A.S. Farghaly, and B. Benmokrane, *Experimental behavior of glass fiber-reinforced polymer-reinforced concrete columns under lateral cyclic load.* ACI Structural Journal, 2018. **115**(2): p. 337-349.
92. Arafa, A., A.S. Farghaly, and B. Benmokrane, *Experimental behavior of GFRP-reinforced concrete squat walls subjected to simulated earthquake load.* Journal of Composites for Construction, 2018. **22**(2): p. 04018003.
93. Deng, Z., L. Gao, and X. Wang, *Glass fiber-reinforced polymer-reinforced rectangular concrete columns under simulated seismic loads.* Journal of the Brazilian Society of Mechanical Sciences and Engineering, 2018. **40**(2): p. 111.